CARDIFF UNIVERSITY
PRIFYSGOL CAERDYDD

ORCA – Online Research @ Cardiff

This is an Open Access document downloaded from ORCA, Cardiff University's institutional repository:https://orca.cardiff.ac.uk/id/eprint/114080/

This is the author's version of a work that was submitted to / accepted for publication.

Citation for final published version:

McDonald, Julie A.K., Mullish, Benjamin H., Pechlivanis, Alexandros, Liu, Zhigang, Brignardello, Jerusa, Kao, Dina, Holmes, Elaine, Li, Jia V., Clarke, Thomas B., Thursz, Mark R. and Marchesi, Julian R. 2018. Inhibiting growth of Clostridioides difficile by restoring valerate, produced by the intestinal microbiota. Gastroenterology 155 (5) , pp. 1495-1507. 10.1053/j.gastro.2018.07.014

Publishers page: http://dx.doi.org/10.1053/j.gastro.2018.07.014

Please note:
Changes made as a result of publishing processes such as copy-editing, formatting and page numbers may not be reflected in this version. For the definitive version of this publication, please refer to the published source. You are advised to consult the publisher's version if you wish to cite this paper.

This version is being made available in accordance with publisher policies. See http://orca.cf.ac.uk/policies.html for usage policies. Copyright and moral rights for publications made available in ORCA are retained by the copyright holders.

Accepted Manuscript

Inhibiting Growth of *Clostridioides difficile* by Restoring Valerate, Produced by the Intestinal Microbiota

Julie A.K. McDonald, Benjamin H. Mullish, Alexandros Pechlivanis, Zhigang Liu, Jerusa Brignardello, Dina Kao, Elaine Holmes, Jia V. Li, Thomas B. Clarke, Mark R. Thursz, Julian R. Marchesi

PII: S0016-5085(18)34771-1
DOI: 10.1053/j.gastro.2018.07.014
Reference: YGAST 61989

To appear in: *Gastroenterology*
Accepted Date: 9 July 2018

Please cite this article as: McDonald JAK, Mullish BH, Pechlivanis A, Liu Z, Brignardello J, Kao D, Holmes E, Li JV, Clarke TB, Thursz MR, Marchesi JR, Inhibiting Growth of *Clostridioides difficile* by Restoring Valerate, Produced by the Intestinal Microbiota, *Gastroenterology* (2018), doi: 10.1053/j.gastro.2018.07.014.

This is a PDF file of an unedited manuscript that has been accepted for publication. As a service to our customers we are providing this early version of the manuscript. The manuscript will undergo copyediting, typesetting, and review of the resulting proof before it is published in its final form. Please note that during the production process errors may be discovered which could affect the content, and all legal disclaimers that apply to the journal pertain.

ACCEPTED MANUSCRIPT

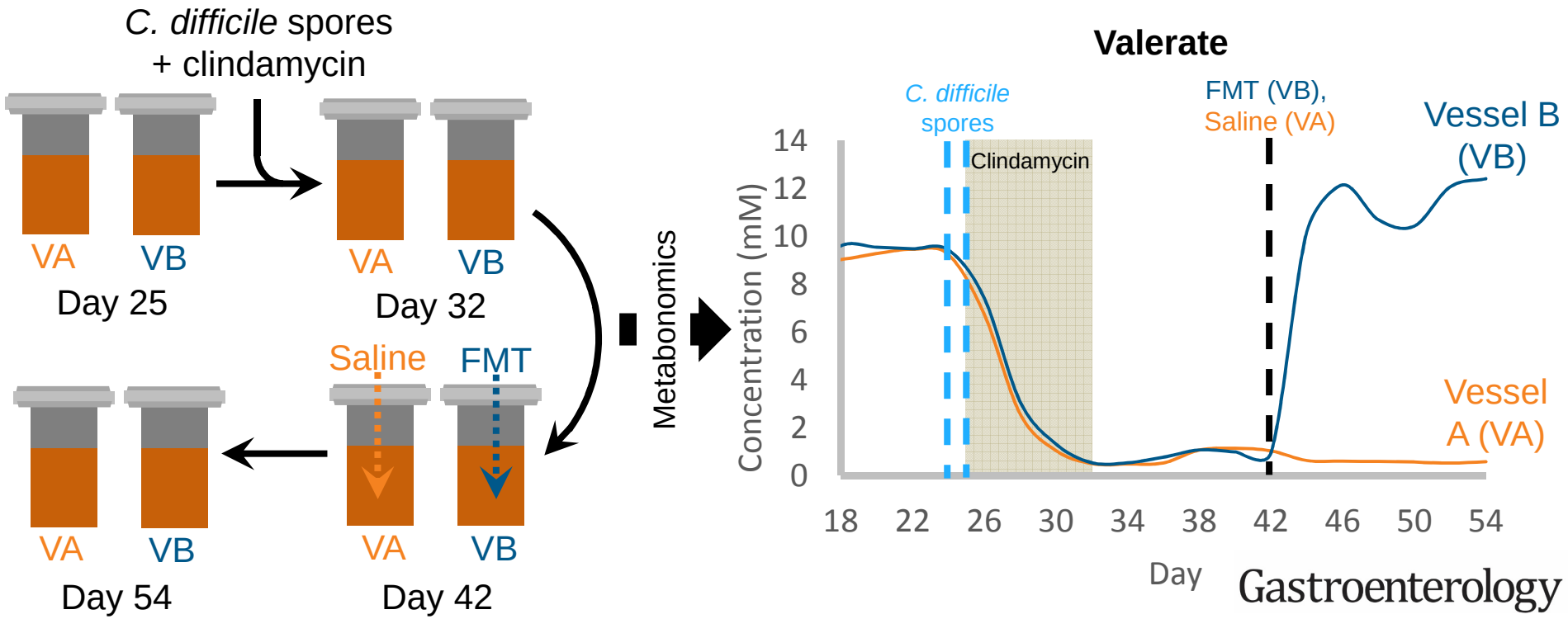

ACCEPTED MANUSCRIPT

Inhibiting Growth of *Clostridioides difficile* by Restoring Valerate, Produced by the Intestinal Microbiota

Short title: Valerate inhibits *Clostridioides difficile*

Julie A. K. McDonald[1], Benjamin H. Mullish[1], Alexandros Pechlivanis[1], Zhigang Liu[1], Jerusa Brignardello[1], Dina Kao[2], Elaine Holmes[1], Jia V. Li[1], Thomas B. Clarke[3], Mark R. Thursz[1], Julian R. Marchesi[1,4]

1. Division of Integrative Systems Medicine and Digestive Disease, Department of Surgery and Cancer, Faculty of Medicine, Imperial College London, London, UK.
2. Division of Gastroenterology, Department of Medicine, University of Alberta, Edmonton, Alberta, Canada.
3. MRC Centre for Molecular Bacteriology and Infection, Imperial College London, London, UK.
4. School of Biosciences, Cardiff University, Cardiff, UK.

Grant support: The Division of Integrative Systems Medicine and Digestive Disease at Imperial College London receives financial support from the National Institute of Health Research (NIHR) Imperial Biomedical Research Centre (BRC) based at Imperial College Healthcare NHS Trust and Imperial College London. This article is independent research funded by the NIHR BRC, and the views expressed in this publication are those of the authors and not necessarily those of the NHS, NIHR, or the Department of Health. BHM is the recipient of a Medical Research Council (MRC) Clinical Research Training Fellowship (grant reference: MR/R000875/1). DK received research funding from Alberta Health Services and University of Alberta Hospital Foundation. TBC is a Sir Henry Dale Fellow jointly funded by the Wellcome Trust and Royal Society (Grant Number 107660/Z/15Z).

Abbreviations: ^{1}H-NMR, proton nuclear magnetic resonance; CA, cholic acid; CDCA, chenodeoxycholic acid; CDI, *Clostridioides difficile* infection; COSY, correlation spectroscopy; DCA, deoxycholic acid; FDR, false discovery rate; FMT, faecal microbiota transplantation; GC-MS, gas chromatography-mass spectrometry; GCA, glycocholic acid; GCDCA, glycochenodeoxycholic acid; GDCA, glycodeoxycholic acid; LCA, lithocholic acid; NOESY, nuclear Overhauser enhancement spectroscopy; OD_{600}, optical density at 600 nm; OTU, operational taxonomic unit; PBS, phosphate buffered saline; rCCA, regularised Canonical Correlation Analysis; SANTA, Short AsyNchronous Time-series Analysis; STOCSY, statistical total correlation spectroscopy; TCA, taurocholic acid; TDCA, taurodeoxycholic acid; TOCSY, total correlation spectroscopy; TVC, total viable counts; UDCA, ursodeoxycholic acid; UPLC-MS, ultra-performance liquid chromatography-mass spectrometry; VA, vessel A; VB, vessel B.

Correspondence:

Prof. Julian R. Marchesi,

Division of Integrative Systems Medicine and Digestive Disease,

Department of Surgery and Cancer, Faculty of Medicine,

Imperial College London, St Mary's Hospital Campus,

South Wharf Road, London, UK W2 1NY,

Tel: +44 02033126197, j.marchesi@imperial.ac.uk or marchesijr@cardiff.ac.uk

Disclosures: DK has received research funding from Rebiotix. All other authors disclose no conflicts.

Author Contributions: JAKM and JRM designed the study. BHM sourced faecal samples and helped with data analysis. JAKM conducted the chemostat experiments, 16S rRNA gene sequencing, 16S rRNA gene qPCR, batch culture experiments, data integration, and performed statistical analysis. JAKM, AP, and BHM performed bile acid UPLC-MS and data analysis. JAKM, JVL, and ZL performed

ACCEPTED MANUSCRIPT

1D- and 2D-NMR and data analysis. DK provided human stool samples for GC-MS analysis. BHM and JB performed GC-MS and data analysis. TBC and JAKM performed the mouse experiments. JAKM wrote the manuscript and all authors edited the manuscript. All authors read and approved the final version of the manuscript.

ACCEPTED MANUSCRIPT

ABSTRACT:

Background & Aims: Fecal microbiota transplantation (FMT) is effective for treating recurrent *Clostridioides difficile* infection (CDI), but there are concerns about its long-term safety. Understanding the mechanisms of the effects of FMT could help us design safer, targeted therapies. We aimed to identify microbial metabolites that are important for *C difficile* growth.

Methods: We used a CDI chemostat model as a tool to study the effects of FMT in vitro. The following analyses were performed: *C difficile* plate counts, 16S rRNA gene sequencing, ^{1}H-NMR spectroscopy, and UPLC mass spectrometry bile acid profiling. FMT mixtures were prepared using fresh fecal samples provided by donors enrolled in an FMT program in the United Kingdom. Results from chemostat experiments were validated using human stool samples, *C difficile* batch cultures, and C57BL/6 mice with CDI. Human stool samples were collected from 16 patients with recurrent CDI and healthy donors (n=5) participating in an FMT trial in Canada.

Results: In the CDI chemostat model, clindamycin decreased valerate and deoxycholic acid concentrations and increased *C difficile* total viable counts (TVC) and valerate precursors, taurocholic acid, and succinate concentrations. After we stopped adding clindamycin, levels of bile acids and succinate recovered, whereas levels of valerate and valerate precursors did not. In the CDI chemostat model, FMT increased valerate concentrations and decreased *C difficile* TVC (94% reduction), spore counts (86% reduction), and valerate precursor concentrations—concentrations of bile acids were unchanged. In stool samples from patients with CDI, valerate was depleted before FMT, but restored after FMT. *C difficile* batch cultures confirmed that valerate decreased vegetative growth, and that taurocholic acid is required for germination but had no effect on vegetative growth. *C difficile* TVC were decreased by 95% in mice with CDI given glycerol trivalerate compared to phosphate-buffered saline.

Conclusions: We identified valerate as a metabolite that is depleted with clindamycin and only recovered with FMT. Valerate is a target for a rationally designed recurrent CDI therapy.

Key words: bacteria; stool transplant; gut microbiome; pathogen

ACCEPTED MANUSCRIPT

INTRODUCTION:

Clostridioides difficile (formerly *Clostridium difficile*) is an anaerobic, spore-forming, Gram-positive bacterium that causes opportunistic infections in the human colon, usually after antibiotic exposure. *C difficile* infection (CDI) can lead to diarrhoea, pseudomembranous colitis, toxic megacolon, intestinal perforation, multi-organ failure, and death.[1] A recent study showed that the incidence of recurrent CDI has disproportionately increased relative to CDI overall, therefore the demand for recurrent CDI therapies may be rising.[2]

The principle behind faecal microbiota transplantation (FMT) is to use stool from a healthy donor to replace the microorganisms and ecosystem functions that are depleted in the gut of recurrent CDI patients. While FMT is highly effective at treating recurrent CDI,[3] it lacks a detailed mechanism of action and it is unclear whether all the microbes included in the preparations are required to resolve disease. There are concerns regarding the long-term safety, reproducibility, composition, and stability of FMT preparations,[4] and potential risks include transmission of infections, invasive administration routes, and concerns treating high-risk individuals (frail/elderly or immunosuppressed patients). In addition, as more studies describe the role of the gut microbiota in disease, it is unclear whether FMT could result in the transfer of a gut microbiota which later contributes to disease (e.g. colorectal cancer, obesity, inflammatory bowel disease, etc).

C difficile causes disease after germination, where cells change from their dormant spore state to their active vegetative state.[5] Previous studies have suggested that exposure to antibiotics alters the composition and functionality of the gut microbiota, changing the global metabolic profile to an environment that supports *C difficile* germination and vegetative growth.[6] Studies have shown that antibiotic exposure and FMT alters many microbial metabolic pathways, including bile acid metabolism[7] and succinate metabolism.[8] In fact, Ott and colleagues showed that sterile faecal filtrate from healthy stool donors was able to cause remission from recurrent CDI in a preliminary investigation of five patients with the condition.[9] It is possible the sterile faecal filtrate contained

bacterial metabolites or enzymes that were sufficient to inhibit *C difficile* spore germination and vegetative growth.

Mechanistic studies are challenging to conduct *in vivo* due to the wide variety of factors which influence the composition and functionality of the gut microbiota. Firstly, samples from recurrent CDI patients prior to FMT are usually collected while they are still on suppressive vancomycin. Therefore, it is difficult to determine whether changes in specific bacteria or metabolites following FMT are due to the FMT administration, or whether these changes could have occurred in the absence of FMT due to recovery of the gut microbiota following cessation of antibiotic treatment. Changes in diet can also cause profound changes in the composition and functionality of the gut microbiota, especially short chain fatty acid production,[10] and diet is especially difficult to control in human studies. Recurrent CDI patients may eat differently before and after receiving FMT, and may eat differently from healthy controls. Studies on diet, the gut microbiota, and short chain fatty acid production have often relied on fermentation data *in vitro* and animal data due to the challenges associated with human studies.[11] Therefore, human studies could lead to "false positives" for mechanisms of *C difficile* pathogenesis.

Data collected from chemostat studies can be used to complement microbiome data collected from human and animal studies to more easily determine a mechanism of action for specific disease states or interventions.[12] Chemostat models are artificial systems that mimic some of the spatial, temporal, and environmental conditions found in the human gut.[13] Chemostats have many advantages over human and animal studies, which have been discussed in detail previously.[12] Bacterial communities cultured in these models are highly reproducible, stable, complex, and representative of the bacterial communities found *in vivo*.[14,15] This means researchers can perform longitudinal studies in these systems that can directly link changes in the gut microbiota structure and function to an experimental intervention. Chemostats have previously been used to model CDI and test the effects of several treatments on *C difficile* growth and pathogenesis (e.g. antibiotics,[16-19] bacteriophages,[20] and lactoferrin[21]).

We used a twin-vessel single-stage distal gut chemostat model as a tool to study CDI and the effects of FMT under tightly-controlled conditions *in vitro*. We hypothesised that exposure to antibiotics kills bacteria that perform important functions in the gut microbial ecosystem, resulting in a "metabolic dysbiosis" where the loss or reduction of specific microbial metabolic pathways creates an environment that promotes *C difficile* germination and growth. We also hypothesised that FMT administration would reverse these effects by restoring the bacteria responsible for performing these key metabolic functions. Our aim was to identify these metabolites so we could propose new therapeutic approaches to treat recurrent CDI that are well-defined, effective, and safe.

MATERIALS AND METHODS:

Chemostat model of CDI:

The chemostat models used in this study were two identical Electrolab FerMac 200 series bioreactor systems (Electrolab, Tewkesbury, UK). Chemostat inoculum and growth medium were prepared and vessels were inoculated and operated as previously described (see Supplementary Methods).[14] Stool samples were collected under approval from the UK National Research Ethics Centres (13/LO/1867). We performed three separate twin-vessel chemostat experiments. In each experiment, two identical vessels ("VA" receiving saline vehicle control and "VB" receiving FMT preparation) were inoculated with a 10% (w/v) faecal slurry prepared using fresh faeces from a healthy donor not exposed to antibiotics within the previous 2 months (Run 1= male in his 40's; Run 2= male in his 60's; Run 3= male in his 80's). We used clindamycin and *C difficile* spores to induce CDI in our chemostat model following a modified version of the methods previously described by Freeman and colleagues (see **Table 1** and Supplementary Methods).[22] After stopping clindamycin dosing, microbial communities were allowed to stabilise before administering the FMT preparation or saline vehicle control. FMT mixtures were prepared using fresh faecal samples provided by donors

enrolled within Imperial's FMT Programme.[23] Stool samples from these faecal donors have previously been used to successfully treat recurrent CDI patients.

16S rRNA gene sequencing (metataxonomics):

DNA extraction is described in the Supplementary Methods. Sample libraries amplifying the V3-V4 region of the 16S rRNA gene were prepared following Illumina's 16S Metagenomic Sequencing Library Preparation Protocol,[24] with a few modifications. First, we used the SequalPrep Normalization Plate Kit (Life Technologies, Carlsbad, USA) to clean up and normalise the index PCR reactions. Also, we used the NEBNext Library Quant Kit for Illumina (New England Biolabs, Ipswich, USA) to quantify the sample libraries. Sequencing was performed on an Illumina MiSeq platform (Illumina Inc, San Diego, USA) using the MiSeq Reagent Kit v3 (Illumina) and paired-end 300 bp chemistry. The resulting data were pre-processed and analysed as described in the Supplementary Methods.

^{1}H-NMR spectroscopy:

Chemostat culture supernatants were prepared for ^{1}H-NMR as described in the Supplementary Methods. One-dimensional ^{1}H-NMR spectra were acquired from chemostat culture supernatants at 300 K on a Bruker DRX 600 MHz NMR spectrometer or a Bruker AVANCE III 600 MHz NMR spectrometer (Bruker Biospin, Germany). A standard one-dimensional NMR pulse sequence [RD-90°-t_1-90°-t_m-90°-acq] was used with a recycle delay (4 s) and mixing time (100 ms). The 90° pulse length was around 10 µs and 32 scans were recorded. Metabolites concentrations were quantified from spectra using the Chenomx NMR suite software (Chenomx Inc, Edmonton, Canada).[25]

To confirm the identity of key metabolites in chemostat culture supernatants a series of NMR spectra including 1D ^{1}H NOESY, 2D ^{1}H–^{1}H TOCSY and ^{1}H–^{1}H COSY of a chemostat culture supernatant and a metabolite standard were recorded (see Supplementary Methods).

Ultra-performance liquid chromatography-mass spectrometry (UPLC-MS) bile acid profiling:

Bile acids were extracted from 50 µL of chemostat culture by adding 150 µL of cold methanol, followed by incubation at -30°C for 2 hours. Tubes were centrifuged at 9500 x g and 4°C for 20 min and 120µL of supernatant was loaded into vials. Bile acid analysis was performed using an ACQUITY UPLC (Waters Ltd, Elstree, UK) coupled to a Xevo G2 Q-ToF mass spectrometer. The MS system was equipped with an electrospray ionization source operating in negative ion mode, using methods previously described by Sarafian and colleagues.[26] Data pre-processing and analysis are described in the Supplementary Methods.

Gas chromatography-mass spectrometry (GC-MS) analysis of human stool samples:

Human stool samples were collected from recurrent CDI patients (n=16) and healthy donors (n=5) as part of a randomised clinical trial comparing the efficacy of capsulized and colonoscopic FMT for the treatment of recurrent CDI, as previously described.[27] Pre-FMT samples were collected from recurrent CDI patients while on suppressive vancomycin. Post-FMT samples were collected 1, 4, and 12 weeks after FMT treatment. All patients were successfully treated following a single FMT.

A targeted GC-MS protocol was used to identify and quantify short chain fatty acids from human stool samples as previously-described.[28] Samples were analysed on an Agilent 7890B GC system, coupled to an Agilent 5977A mass selective detector (Agilent, Santa Clara, CA). Data analysis was performed using MassHunter software (Agilent).

***C difficile* batch cultures:**

We tested the effects of valerate (Fisher Scientific) on the vegetative growth of three *C difficile* ribotypes (010, 012, and 027) as well as several gut commensal bacteria (*Bacteroides uniformis*, *Bacteroides vulgatus*, and *Clostridium scindens*) (see Supplementary Methods). We centrifuged an overnight culture of the test isolate at 3000 x g for 10 minutes and resuspended the cells in brain heart infusion broth (Sigma-Aldrich) (supplemented with 5 mg/mL yeast extract (Sigma-Aldrich), and

0.1% L-cysteine (Sigma-Aldrich)), containing varying concentrations of valerate (0, 1, 2, 3, 4, 5, 10, and 20 mM, pH of broth adjusted to 6.8) in triplicate. The OD_{600} was measured at time zero and cultures were incubated at 37°C in an ElectroTek AW 400TG Anaerobic Workstation (ElectroTek, West Yorkshire, UK). Additional OD_{600} measurements were taken at 2, 4, 6, and 8 hours post-inoculation. We plotted the changes in OD_{600} (from a time point during the exponential phase) against each concentration of valerate tested. We used ANOVA and Tukey post hoc test to determine whether the concentration of valerate tested affected the growth of the test isolate compared to batch cultures grown in the absence of valerate.

We also tested the effects of taurocholic acid (TCA) on *C difficile* germination and vegetative growth using batch cultures (see Supplementary Methods).

Mouse model of CDI:

Mouse experiments were performed under the authority of the UK Home Office outlined in the Animals (Scientific Procedures) Act 1986 after ethical review by Imperial College London Animal Welfare and Ethical Review Body (PPL 70/7969). We adhered to standards articulated in the Animal Research: Reporting of *In Vivo* Experiments (ARRIVE) guidelines.

Wild-type C57BL/6 mice (8-10-week-old; female) were purchased from Envigo (UK) and acclimatised for 1 week prior to use. Mice were housed five per cage in individually ventilated cages with autoclaved food (RM1, Special Diet Services), bedding (Aspen chip 2 bedding), and water (provided *ad libitum*). Mice were subjected to a 12 h light and 12 h dark cycle at 20–22°C.

We used a previously published mouse model of *C difficile* infection as described by Winston and colleagues (**Figure 6A**).[29] Briefly, mice were given 0.5 mg/ml cefoperazone in their drinking water for 5 days (from day -7 to day -2), followed by autoclaved antibiotic-free water for the remainder of the experiment. *C difficile* spores were prepared and enumerated (see Supplementary Methods) and mice were challenged with 10^5 *C difficile* spores by oral gavage on day 0. Mice were orally gavaged with 200 µl of 15 mM glycerol trivalerate (n=5) or 200 µl of PBS (n=5) on days 1, 2, and 3. Faecal

samples were collected on days 1, 2, 3, and 4 and *C difficile* total viable counts (TVC) were quantified (see Supplementary Methods). Mice were not fasted before oral gavages and all interventions were performed during the light cycle.

Statistical analysis and data integration:

Statistical tests were performed using IBM SPSS Statistics Software version 23 (paired t-test, independent t-test, ANOVA) or GraphPad Prism version 7.03 (Mann-Whitney U test, Friedman test). Short AsyNchronous Time-series Analysis (SANTA) was used to determine whether there were significant changes in data trajectories at several time periods over the course of the chemostat experiments (see Supplementary Methods).[30] Spearman's *rho* statistic and p-values were calculated for *C difficile* TVC and metabolite data using the cor and cor.test functions, respectively, within the stats base library within R. A p-value less than 0.05 was considered significant. We used regularised Canonical Correlation Analysis (rCCA) to correlate metataxonomic and metabolomic data using the mixOmics library within R (see Supplementary Methods).[31]

RESULTS:

***C difficile* total viable counts and spore counts from chemostat culture samples:**

Following the addition of *C difficile* spores to each vessel *C difficile* TVC and spore counts were enumerated every other day until the end of the experiment (**Figure 1**). We found an increase in *C difficile* TVC during the clindamycin-dosing period ($p<0.001$). We also found a 94% reduction in *C difficile* TVC ($p=0.025$) and an 86% reduction in *C difficile* spore counts ($p=0.034$) in FMT-treated cultures compared to saline-treated cultures.

Bacterial community composition of chemostat culture samples:

We found that clindamycin dosing of chemostat cultures altered the composition and the biomass of the bacterial communities (**Figure S1**). Clindamycin dosing caused an initial decrease in

the total bacterial biomass one day after starting clindamycin dosing (p<0.001), however the total bacterial biomass increased over time to reach pre-clindamycin levels by the end of the clindamycin dosing period (p>0.05). Clindamycin dosing also resulted in a decrease in bacterial diversity (p=0.002), richness (the number of species present, p=0.001) and evenness (how evenly distributed each species is, p=0.004) (**Figure S2**). There was a significant increase in richness following FMT treatment (p=0.035), however diversity (p>0.05) and evenness (p>0.05) remained unchanged.

Global metabolic profiling of chemostat culture samples by ^{1}H-NMR spectroscopy:

We performed ^{1}H-NMR spectroscopy as an exploratory technique to generate global metabolite spectral profiles for samples collected over the course of the chemostat experiments. There was a significant decrease in valerate (p=0.004), butyrate (p=0.004), and acetate (p=0.013) and a significant increase in 5-aminovalerate (p=0.004), ethanol (p=0.021), succinate (p=0.004), and isobutyrate (p=0.004) during the clindamycin dosing period compared to the steady state period (**Figures 2 and S3**). rCCA modelling was used to determine correlations between 16S rRNA gene sequencing data and metabolite data that correspond to clindamycin dosing. The unit representation plot showed a clear separation between steady state cultures and cultures sampled during and after the clindamycin dosing period (**Figure S4A**). The correlation circle plot showed that the separation between the cultures was due to decreases in the levels of valerate and acetate, and increases in the levels 5-aminovalerate, succinate, isobutyrate, and ethanol during and after the clindamycin dosing period (**Figure S4B**). This plot also showed strong correlations between bacterial genera and these metabolites. During the clindamycin-dosing period there were significant correlations between *C difficile* TVC and valerate (r_S=-0.59, p=0.005), 5-aminovalerate (r_S=0.54, p=0.010), and succinate (r_S=-0.49, p=0.022).

Following the end of the clindamycin-dosing period the levels of succinate, butyrate, acetate, and isobutyrate recovered to pre-antibiotic levels, and these levels were not affected by FMT treatment (**Figures 2 and S3**). However, after stopping clindamycin dosing the levels of valerate (p=0.009) were

still significantly decreased and the levels of 5-aminovalerate (p=0.009) and ethanol (p=0.013) were still significantly increased compared to pre-antibiotic levels (**Figure 2**), indicating the levels of these metabolites did not recover after stopping clindamycin dosing. Moreover, after stopping clindamycin dosing the levels of isovalerate decreased (p=0.009) and the levels of propionate increased (p=0.036) compared to pre-antibiotic levels (**Figures 2 and S3**).

There was a significant increase in valerate (p=0.032), and significant decreases in 5-aminovalerate (p=0.032), ethanol (p=0.032), propionate (p=0.032), and methanol (p=0.039) in FMT-treated cultures compared to saline-treated cultures (**Figure 2**). rCCA modelling was also used to determine correlations between 16S rRNA gene sequencing data and metabolite data that correspond to FMT or saline treatment. The unit representation plot showed a clear separation between FMT-treated cultures and saline-treated cultures along the second canonical variate (**Figure S4C**). The correlation circle plot showed that the separation between FMT- and saline-treated cultures was due to increases in the levels of valerate and decreases in the levels of 5-aminovalerate, ethanol, and methanol in FMT-treated cultures (**Figure S4D**). This plot also showed strong correlations between bacterial genera and these metabolites. Following FMT or saline treatment there was a significant strong negative correlation between *C difficile* TVC and valerate (r_S=-0.67, p=1.48x10^{-4}), and significant strong positive correlations between *C difficile* TVC and 5-aminovalerate (r_S=0.76, p=6.07x10^{-6}), ethanol (r_S=0.81, p=1.72x10^{-6}), and methanol (r_S=0.72, p=2.98x10^{-5}).

The identity of the proposed valerate peaks was confirmed in the chemostat culture supernatants by performing 1D-^{1}H-NMR spectroscopy of a sample before and after valerate spike-in, as well as 2D-^{1}H-NMR spectroscopy of a valerate-containing sample (**Figures S5 and S6**, Supplementary Results). The identities of other metabolites were also confirmed in the chemostat culture supernatants by performing 2D-^{1}H-NMR and STOCSY (**Figures S7 and S8**).

Bile acid UPLC-MS profiling of chemostat culture samples:

Due to the important role that bile acids play in *C difficile* spore germination and vegetative growth,[5] we also measured changes in bile acids over the course of the chemostat experiments. During the clindamycin dosing period there was a significant increase in the conjugated primary bile acids taurocholic acid (TCA, p=0.004), glycocholic acid (GCA, p=0.005), and glycochenodeoxycholic acid (GCDCA, p=0.005), in the unconjugated primary bile acids cholic acid (CA, p=0.004) and chenodeoxycholic acid (CDCA, p=0.037), and in the conjugated secondary bile acids taurodeoxycholic acid (TDCA, p=0.045) and glycodeoxycholic acid (GDCA, p=0.004) (**Figures 3 and S9**). During the clindamycin dosing period there was a significant decrease in the secondary bile acids deoxycholic acid (DCA, p=0.006), lithocholic acid (LCA, p=0.005), and ursodeoxycholic acid (UDCA, p=0.037) (**Figures 3 and S9**). Following the end of the clindamycin dosing period the levels of these bile acids recovered to steady state levels (before clindamycin dosing), and these levels were not affected by FMT treatment.

rCCA modelling was used to determine correlations between 16S rRNA gene sequencing data and bile acid data during the clindamycin-dosing period. The unit representation plot showed separation between cultures sampled before and during the clindamycin-dosing period along the first canonical variate, but no separation between cultures sampled before and after the clindamycin-dosing period (**Figure S10A**). The correlation circle plot showed that the separation between cultures sampled before and during clindamycin dosing was due to increases in the levels of TCA, CA, CDCA, GCA, GDCA, and GCDCA, and decreases in the levels of DCA, LCA, and UDCA during the clindamycin-dosing period (**Figure S10B**). This plot also showed strong correlations between bacterial genera and bile acids.

There were significant strong correlations between *C difficile* TVC and several bile acids during the clindamycin dosing period, including TCA (r_S=0.68, p=6.29x10^{-4}), CA (r_S=0.61, p=0.003), DCA (r_S=-0.75, p=8.86x10^{-5}), and LCA (r_S=-0.76, p=6.36x10^{-5}).

GC-MS analysis of human stool samples:

To confirm the findings from our chemostat experiments we measured the levels of valerate in human stool samples from healthy FMT donors, recurrent CDI patients pre-FMT and at several time points post-successful FMT (1, 4, and 12 weeks after FMT treatment) (**Figure 4**). Valerate was depleted in stool samples from recurrent CDI patients pre-FMT compared to healthy donors (p=0.0075). Valerate levels were significantly increased in CDI patients post-FMT compared to pre-FMT (p=0.0007 at 1 week, 4 weeks, and 12 weeks). There were no significant differences in the levels of valerate in stool samples from healthy donors compared to any of the time points from CDI patients collected post-FMT (p>0.05 for all comparisons).

***C difficile* batch culture experiments with valerate and TCA:**

Batch culture experiments were performed to directly study the effects of specific metabolites of interest on *C difficile* germination and vegetative growth and to confirm the findings from our chemostat experiments. These experiments showed that valerate inhibited the vegetative growth *C difficile* ribotype 010 at concentrations ≥ 4 mM (p=0.008), ribotype 012 at concentrations ≥ 2 mM (p=0.003), and ribotype 027 at concentrations ≥ 2 mM (p=0.008) (**Figure 5**). The concentration of valerate in FMT-treated chemostat culture supernatants remained above 4 mM for all samples, whereas the concentration of valerate in saline-treated cultures remained below 2 mM for all samples. As a control, we also tested the effects of valerate on commensal gut isolates (*B uniformis* and *B vulgatus*, two representatives of *Bacteroidetes*, and *C scindens*, a representative of *Firmicutes*). *B uniformis* was only inhibited in broth containing 20 mM valerate (p=0.026). *B vulgatus* was not inhibited at any concentration of valerate that was tested, and showed more growth in broths containing 10 mM (p=0.020) or 20 mM (p=0.019) valerate. *C scindens* was not inhibited at any concentration of valerate tested (p>0.05 for all concentrations of valerate tested).

Batch culture experiments also confirmed previous findings showing that TCA is required for *C difficile* spore germination but had no effect on vegetative growth (**Figure S11**).

Glycerol trivalerate intervention study in a CDI mouse model:

Next, we determined whether valerate could inhibit *C difficile* growth when administered as an intervention in a CDI mouse model (**Figure 6A**). To avoid the rapid uptake of valerate and obtain sufficient release in the gastrointestinal tract, valerate was administered to the mice in the form of glycerol trivalerate (which is hydrolysed by lipases to release valerate[32]). One-day post-infection (prior to glycerol trivalerate or PBS administration) there was no significant difference in the levels of *C difficile* TVC in mouse faeces in each group (p=0.584). Glycerol trivalerate or PBS was administered to *C difficile*-infected mice by oral gavage 1, 2, and 3 days post-infection (n=5 per group). There was a significant decrease in *C difficile* TVC in glycerol trivalerate-treated mice compared to PBS-treated mice (**Figure 6B**, p=0.027 on day 2, p=0.007 on day 3, and p=0.024 on day 4). After only 3 doses of glycerol trivalerate or PBS, glycerol trivalerate-treated mice had an average of 95% less *C difficile* TVC per gram of faeces compared to PBS-treated mice. No adverse effects were noted in glycerol trivalerate-treated mice over the course of the experiment. These results corroborate the other findings presented in this study and support the therapeutic use of valerate to treat CDI.

DISCUSSION:

We used several 'omic' techniques to study the effects of FMT on CDI in a chemostat model under tightly controlled conditions. The aim of our study was to directly link changes in *C difficile* counts to changes in the structure and function of the cultured faecal microbiota. We confirmed our findings by analysing human stool samples, performing *C difficile* batch culture experiments, and performing an interventional study in a CDI mouse model. A summary of the key findings and proposed interactions between *C difficile*, valerate, and TCA are outlined in **Figure S12**.

In our study we found valerate significantly inhibited the growth of *C difficile*, both *in vitro* and *in vivo*. Valerate is a short chain fatty acid produced via amino acid fermentation by members of the gut microbiota.[33] Valerate was significantly depleted in chemostat culture samples during clindamycin dosing and did not recover after clindamycin dosing was stopped. Valerate significantly

increased with FMT treatment and had a strong negative correlation with *C difficile* TVC. These findings were corroborated with human data which showed valerate was depleted in recurrent CDI patient stool but was restored following successful FMT. Batch culture experiments confirmed that valerate directly inhibited the vegetative growth of several *C difficile* ribotypes, but had minimal effects on the growth of other commensal gut bacteria tested. Moreover, we showed that glycerol trivalerate significantly decreased *C difficile* TVC in a CDI mouse model. We hypothesise that maintaining or restoring the levels of valerate in the gut microbiota of CDI patients will inhibit the vegetative growth of *C difficile*. This restoration could be accomplished by directly supplying the gut with valerate (e.g. in the form of glycerol trivalerate) or by administering bacteria capable of transforming valerate precursors into to valerate.

There are several different metabolic pathways that lead to valerate production. 5-aminovalerate is a product of the anaerobic degradation of protein hydrolysates by members of the gut microbiota, in particular *Clostridium* species.[34] In this pathway, proline is reduced to 5-aminovalerate by proline reductase in a Stickland-type fermentation.[35-37] 5-aminovalerate is then fermented to valerate in a series of reactions mediated by gut bacteria.[34,38] We showed that 5-aminovalerate was increased in chemostat cultures following clindamycin dosing and remained increased after clindamycin dosing was stopped. This finding is supported by data from a patent submitted by Savidge and Dann, who proposed CDI patients can be distinguished from non-infected subjects by measuring elevated levels of 5-aminovalerate in the patient's stool, urine, or blood.[39] Moreover, Fletcher and colleagues showed that 5-aminovalerate was elevated in the caecal content of *C difficile* infected mice.[40] In another metabolic pathway, some *Clostridium* species can ferment ethanol and propionate to valerate.[41] We found ethanol and propionate increased after clindamycin dosing and decreased following FMT treatment. Taken together, changes in the levels of valerate and valerate precursors (5-aminovalerate, ethanol, and propionate) over the course of our chemostat experiments supports our hypothesis that disruption of the valerate pathway due to antibiotics results in an environment that permits *C difficile* vegetative growth.

In this study we performed an intervention experiment to test the effects of valerate (in the form of glycerol trivalerate) in a CDI mouse model. For the first time we showed that glycerol trivalerate-treated mice had significantly reduced *C difficile* TVC compared to PBS-treated control mice (95% reduction in glycerol-trivalerate treated mice after 3 doses). The results from our study are consistent with the previously published study by Theriot and colleagues, who briefly mention that antibiotic-exposed mice (who were susceptible to CDI) had a 66-fold decrease in valerate compared to non-antibiotic controls (who were resistant to CDI).[6] They also showed that antibiotic-exposed mice had increased levels of amino acids required for *C difficile* growth (including proline, a precursor to 5-aminovalerate) compared to non-antibiotic controls. Six weeks later, antibiotic-exposed mice were fully-resistant to CDI following exposure to *C difficile* spores. As shown in the supplementary material of their paper, Theriot and colleagues found that valerate levels had partially recovered six weeks later, and were only 4.9-fold decreased in antibiotic-exposed mice compared to non-antibiotic controls.

C difficile spores can persist following the cessation of antibiotics and germinate to vegetative cells which initiate disease relapse. In our study we found that TCA, a known potent germinant for *C difficile* spores,[5] was increased during clindamycin dosing, remained elevated for several days after stopping clindamycin, and had a strong positive correlation with *C difficile* TVC. However, after stopping clindamycin and allowing chemostat communities to recover and stabilise, we found that bile acid levels recovered to pre-clindamycin levels and did not change with FMT treatment. We hypothesise that the transient increase in TCA found during and shortly after stopping clindamycin dosing stimulated *C difficile* spore germination, resulting in vegetative growth. Once clindamycin dosing stopped and the levels of TCA decreased to pre-clindamycin levels, *C difficile* spores had already germinated and were growing in their vegetative state which is no longer affected by the presence of TCA (as shown by Sorg and Sonnenshein[5], and confirmed in our study using batch cultures). These results are also consistent with the previously published study by Theriot and colleagues, who showed that antibiotic-exposed mice (who were susceptible to CDI) had a 15-fold

increase in TCA compared to non-antibiotic controls (who were resistant to CDI).[6] Six weeks later (when antibiotic-exposed mice were fully-resistant to CDI) the levels of TCA in antibiotic-exposed mice recovered to the levels found in non-antibiotic controls, suggesting there was insufficient levels of TCA to stimulate *C difficile* germination. Further discussion of bile acid data is included in the Supplementary Discussion.

The first line of therapy for an initial episode of CDI is vancomycin/metronidazole therapy. These antibiotics kill *C difficile* vegetative cells, but *C difficile* spores can persist.[42] If vancomycin/metronidazole therapy is stopped while these *C difficile* spores are present, the elevated levels of TCA (present following the cessation of antibiotics) will cause *C difficile* spore germination, and low levels of valerate will allow *C difficile* vegetative growth and therefore recurrent disease. To prevent CDI initiation and relapse following the cessation of antibiotics, it is also important to maintain low levels of TCA in the gut. One way to accomplish this would be to ensure the maintenance of bile salt hydrolase enzymes during and after antibiotic exposure. These enzymes are produced by commensal gut bacteria and are responsible for deconjugating tauro- and glyco-conjugated bile acids. It has been proposed that antibiotics kill bile salt hydrolase-producing bacteria, resulting in the accumulation of TCA in the gut. Therefore, re-inoculation of bile salt hydrolase-producing bacteria with FMT may be responsible for degrading TCA present following the cessation of antibiotics, and prevent the germination of *C difficile* spores. A more controlled method of restoring bile salt hydrolase activity in the gut microbiomes of CDI patients could be to avoid the administration of live microorganisms by administering purified bile salt hydrolase enzyme preparations.

We also found that succinate transiently increased in chemostat cultures with clindamycin dosing, but negatively correlated with *C difficile* TVC. We believe the negative correlation between *C difficile* TVC and succinate is because *C difficile* uses succinate for growth. A study by Ferreyra and colleagues found that succinate was present at low levels in the guts of healthy mice, but transiently increased with antibiotics or motility disturbance.[8] They found that *C difficile* can metabolise

succinate to butyrate, and it exploits the increase in succinate to grow in perturbed gut microbiota. Again, these findings are consistent with our findings from chemostat experiments. Members of *Bacteroidetes* and the *Negativicutes* class of *Firmicutes* can degrade succinate to propionate, and as such succinate does not usually accumulate to high levels in the guts of healthy humans.[43] Another strategy to give *C difficile* vegetative cells a competitive disadvantage would be to maintain succinate metabolism during antibiotic exposure by administering succinate-degrading enzymes, so succinate is no longer available for *C difficile* growth.

The findings from our study support the hypothesis that antibiotic exposure causes a depletion of specific metabolic pathways normally found in healthy gut microbiotas, resulting in a metabolite environment that favours *C difficile* germination and growth. It also supports our hypothesis that FMT administration reverses these effects by restoring the bacteria responsible for performing these key metabolic functions. These findings have the potential to directly impact clinical practice in the foreseeable future by developing targeted treatments for CDI by different routes, alone or in combinations: (1) directly supplement the gut with valerate (to inhibit *C difficile* vegetative growth); (2) directly supplement the gut with bile salt hydrolase enzymes (to degrade taurocholic acid and prevent *C difficile* spore germination); and (3) directly supplement the gut with succinate-degrading enzymes (to degrade succinate and give *C difficile* vegetative cells a competitive disadvantage). These proposed interventions are well-defined and represent safer options that will avoid all the risks involved with administering live microorganisms to patients and will not promote antimicrobial resistance.

The advantage of using valerate (instead of live microorganisms or relatively undefined FMT preparations) is that valerate is a well-defined small molecule that is normally present in the healthy gut. Valerate may be a preferred treatment for CDI in immunocompromised patients where administration of bacteria may increase the risk of a subsequent infection, or in CDI patients that require further antibiotic treatment for other purposes (where the antibiotic treatment would kill bacteria present in FMT preparations and render the treatment less effective). Valerate could also

be delivered using more patient-friendly methods that do not require the need to preserve live microorganisms. In this study glycerol trivalerate was orally gavaged to mice, but it has also been included as an additive in animal feed. Therefore, valerate has the potential to be administered to patients via a less invasive route compared to FMT. This promising new therapy merits further evaluation in prospective studies *in vivo*.

REFERENCES:

1. Mitu-Pretorian OM, Forgacs B, Qumruddin A, *et al*. Outcomes of patients who develop symptomatic *Clostridium difficile* infection after solid organ transplantation. Transplant Proc 2010;42:2631-2633.
2. Ma GK, Brensinger CM, Wu Q, *et al*. Increasing incidence of multiply recurrent *Clostridium difficile* infection in the united states: a cohort study. Ann Intern Med 2017;167:152-158.
3. van Nood E, Vrieze A, Nieuwdorp M, *et al*. Duodenal infusion of donor feces for recurrent *Clostridium difficile*. N Engl J Med 2013;368:407-415.
4. **Petrof EO, Gloor GB**, Vanner SJ, *et al*. Stool substitute transplant therapy for the eradication of *Clostridium difficile* infection: 'RePOOPulating' the gut. Microbiome 2013;1:3-2618-1-3.
5. Sorg JA, Sonenshein AL. Bile salts and glycine as cogerminants for *Clostridium difficile* spores. J Bacteriol 2008;190:2505-2512.
6. Theriot CM, Koenigsknecht MJ, Carlson PE,Jr, *et al*. Antibiotic-induced shifts in the mouse gut microbiome and metabolome increase susceptibility to *Clostridium difficile* infection. Nat Commun 2014;5:3114.
7. **Weingarden AR**, **Chen C**, Bobr A, *et al*. Microbiota transplantation restores normal fecal bile acid composition in recurrent *Clostridium difficile* infection. Am J Physiol Gastrointest Liver Physiol 2014;306:G310-9.
8. Ferreyra JA, Wu KJ, Hryckowian AJ, *et al*. Gut microbiota-produced succinate promotes *C difficile* infection after antibiotic treatment or motility disturbance. Cell Host Microbe 2014;16:770-777.

9. **Ott SJ**, **Waetzig GH**, **Rehman A**, *et al*. Efficacy of sterile fecal filtrate transfer for treating patients with *Clostridium difficile* infection. Gastroenterology 2017;152:799-811.e7.

10. De Filippo C, Cavalieri D, Di Paola M, *et al*. Impact of diet in shaping gut microbiota revealed by a comparative study in children from Europe and rural Africa. Proc Natl Acad Sci USA 2010;107:14691-14696.

11. Morrison DJ, Preston T. Formation of short chain fatty acids by the gut microbiota and their impact on human metabolism. Gut Microbes 2016;7:189-200.

12. McDonald JAK. *In vitro* models of the human microbiota and microbiome. Emerging Topics in Life Sciences 2017;1:373-384.

13. Macfarlane GT, Macfarlane S. Models for intestinal fermentation: association between food components, delivery systems, bioavailability and functional interactions in the gut. Curr Opin Biotechnol 2007;18:156-162.

14. McDonald JA, Schroeter K, Fuentes S, *et al*. Evaluation of microbial community reproducibility, stability and composition in a human distal gut chemostat model. J Microbiol Methods 2013;95:167-174.

15. Van den Abbeele P, Grootaert C, Marzorati M, *et al*. Microbial community development in a dynamic gut model is reproducible, colon region specific, and selective for *Bacteroidetes* and *Clostridium* cluster IX. Appl Environ Microbiol 2010;76:5237-5246.

16. Freeman J, Baines SD, Jabes D, *et al*. Comparison of the efficacy of ramoplanin and vancomycin in both *in vitro* and *in vivo* models of clindamycin-induced *Clostridium difficile* infection. J Antimicrob Chemother 2005;56:717-725.

17. Baines SD, O'Connor R, Saxton K, *et al*. Comparison of oritavancin versus vancomycin as treatments for clindamycin-induced *Clostridium difficile* PCR ribotype 027 infection in a human gut model. J Antimicrob Chemother 2008;62:1078-1085.

18. Chilton CH, Crowther GS, Freeman J, *et al*. Successful treatment of simulated *Clostridium difficile* infection in a human gut model by fidaxomicin first line and after vancomycin or metronidazole failure. J Antimicrob Chemother 2014;69:451-462.

19. Chilton CH, Crowther GS, Baines SD, *et al*. *In vitro* activity of cadazolid against clinically relevant *Clostridium difficile* isolates and in an *in vitro* gut model of *C difficile* infection. J Antimicrob Chemother 2014;69:697-705.

20. Meader E, Mayer MJ, Steverding D, *et al*. Evaluation of bacteriophage therapy to control *Clostridium difficile* and toxin production in an *in vitro* human colon model system. Anaerobe 2013;22:25-30.

21. Chilton CH, Crowther GS, Spiewak K, *et al*. Potential of lactoferrin to prevent antibiotic-induced *Clostridium difficile* infection. J Antimicrob Chemother 2016;71:975-985.

22. Freeman J, Baines SD, Saxton K, *et al*. Effect of metronidazole on growth and toxin production by epidemic *Clostridium difficile* PCR ribotypes 001 and 027 in a human gut model. J Antimicrob Chemother 2007;60:83-91.

23. Mullish BH, Marchesi JR, Thursz MR, *et al*. Microbiome manipulation with faecal microbiome transplantation as a therapeutic strategy in *Clostridium difficile* infection. QJM 2015;108:355-359.

24. Illumina I. 16S Metagenomic Sequencing Library Preparation (Part # 15044223 Rev. B); 2013. Available at: https://support.illumina.com/content/dam/illumina-support/documents/documentation/chemistry_documentation/16s/16s-metagenomic-library-prep-guide-15044223-b.pdf, 2017.

25. Weljie AM, Newton J, Mercier P, *et al*. Targeted profiling: quantitative analysis of ^{1}H NMR metabolomics data. Anal Chem 2006;78:4430-4442.

26. **Sarafian MH**, **Lewis MR**, Pechlivanis A, *et al*. Bile acid profiling and quantification in biofluids using ultra-performance liquid chromatography tandem mass spectrometry. Anal Chem 2015;87:9662-9670.

27. Kao D, Roach B, Silva M, *et al.* Effect of oral capsule- vs colonoscopy-delivered fecal microbiota transplantation on recurrent *Clostridium difficile* infection: a randomized clinical trial. JAMA 2017;318:1985-1993.

28. Garcia-Villalba R, Gimenez-Bastida JA, Garcia-Conesa MT, *et al*. Alternative method for gas chromatography-mass spectrometry analysis of short-chain fatty acids in faecal samples. J Sep Sci 2012;35:1906-1913.

29. Winston JA, Thanissery R, Montgomery SA, *et al*. Cefoperazone-treated mouse model of clinically-relevant *Clostridium difficile* strain R20291. J Vis Exp 2016;(118). doi:10.3791/54850.

30. Wolfer A. SANTA-App: Interactive package for Short AsyNchronous Time-series Analysis (SANTA) in R, implemented in Shiny; 2017. Available at: https://github.com/adwolfer/SANTA-App, 2017.

31. Le Cao K, Rohart F, Gonzalez I, *et al*. mixOmics: Omics Data Integration Project. R package version 6.1.2.; 2017. Available at: https://CRAN.R-project.org/package=mixOmics, 2017.

32. Schwartz B. The effect of temperature on the rate of hydrolysis of triglycerides by pancreatic lipase. J Gen Physiol 1943;27:113-118.

33. Neis EP, Dejong CH, Rensen SS. The role of microbial amino acid metabolism in host metabolism. Nutrients 2015;7:2930-2946.

34. Barker HA, D'Ari L, Kahn J. Enzymatic reactions in the degradation of 5-aminovalerate by *Clostridium aminovalericum*. J Biol Chem 1987;262:8994-9003.

35. Seto B, Stadtman TC. Purification and properties of proline reductase from *Clostridium sticklandii*. J Biol Chem 1976;251:2435-2439.

36. Hodgins DS, Abeles RH. Studies of the mechanism of action of D-proline reductase: the presence on covalently bound pyruvate and its role in the catalytic process. Arch Biochem Biophys 1969;130:274-285.

37. Seto B. The Stickland reaction. In: Knowles CJ, ed. Diversity of Bacterial Respiratory Systems (Vol. II). Boca Raton, FL: CRC Press, 1980:49-64.

38. Buckel W. Unusual enzymes involved in five pathways of glutamate fermentation. Appl Microbiol Biotechnol 2001;57:263-273.

39. Savidge T, Dann S. Methods and uses for metabolic profiling for *Clostridium difficile* infection. 2013;PCT/US2012/064218.

40. Fletcher JR, Erwin S, Lanzas C, *et al*. Shifts in the gut metabolome and *Clostridium difficile* transcriptome throughout colonization and infection in a mouse model. mSphere 2018;3:10.1128/mSphere.00089-18. eCollection 2018 Mar-Apr.

41. Bornstein BT, Barker HA. The energy metabolism of *Clostridium kluyveri* and the synthesis of fatty acids. J Biol Chem 1948;172:659-669.

42. Borody TJ, Khoruts A. Fecal microbiota transplantation and emerging applications. Nat Rev Gastroenterol Hepatol 2011;9:88-96.

43. Louis P, Flint HJ. Formation of propionate and butyrate by the human colonic microbiota. Environ Microbiol 2017;19:29-41.

Author names in bold designate shared co-first authorship.

FIGURE LEGENDS:

Figure 1: Average *C difficile* plate counts taken from VA (saline-treated cultures, black dashed line) and VB (FMT-treated cultures, black solid line) over the course of the experiment. **(A)** Average *C difficile* total viable counts. **(B)** Average *C difficile* spore plate counts. The grey shaded box indicates the clindamycin-dosing period, while the vertical dotted line indicates the day of FMT or saline dosing. Error bars represent the mean ± standard deviation (*, $p<0.05$ by SANTA analysis).

Figure 2: ^{1}H-NMR metabolites that changed following clindamycin treatment and with FMT (VA= saline-treated cultures, dashed line; VB= FMT-treated cultures, solid line). **(A)** valerate, **(B)** 5-aminovalerate, **(C)** ethanol, **(D)** succinate, **(E)** propionate, and **(F)** methanol. The shaded grey box indicates the clindamycin-dosing time period, while the vertical dotted line indicates the day of FMT

or saline dosing. SANTA analysis with Benjamini-Hochberg FDR was used to compare the following: steady state cultures to clindamycin-treated cultures, steady state cultures to post-clindamycin cultures, and FMT-treated cultures to saline treated cultures.

Figure 3: Bile acids that changed following clindamycin treatment and correlated with *C difficile* TVC (VA= saline-treated cultures, dashed line; VB= FMT-treated cultures, solid line). **(A)** taurocholic acid (TCA), **(B)** cholic acid (CA), **(C)** deoxycholic acid (DCA), and **(D)** lithocholic acid (LCA). The shaded grey box indicates the clindamycin-dosing period, while the vertical dotted line indicates the day of FMT or saline dosing. Steady state cultures were compared to clindamycin-treated cultures using SANTA analysis with Benjamini-Hochberg FDR.

Figure 4: Effect of FMT on the concentration of valerate in stool from healthy FMT donors (n=5) and recurrent CDI patients pre-FMT (n=16) and at several time points post-FMT (n=16). Mann-Whitney U test for donors vs. pre-FMT, Friedman test for pre-FMT vs. post-FMT. ** p<0.01, *** p<0.001.

Figure 5: Valerate inhibits *C difficile* vegetative growth in batch cultures. Vegetative cells were inoculated into supplemented brain heart infusion broth containing varying concentrations of valerate (0, 1, 2, 3, 4, 5, 10, and 20 mM) and OD_{600} measurements were taken at 0, 2, 4, 6, and 8 hours. The change in OD_{600} (from a time point during the exponential phase) was plotted against the concentrations of valerate tested. **(A)** *C difficile* ribotype 010, **(B)** *C difficile* ribotype 012, **(C)** *C difficile* ribotype 027, **(D)** *B. uniformis*, **(E)** *B. vulgatus,* **(F)** *C. scindens*. Error bars represent the mean ± standard deviation, * p<0.05, ** p<0.01, *** p<0.001.

Figure 6: Glycerol trivalerate significantly reduced faecal *C. difficle* total viable counts in a CDI mouse model. **(A)** Experimental design. Mice were given cefoperazone in their drinking water for 5 days, then switched to antibiotic-free autoclaved water for the remainder of the experiment. On day 0 mice were orally gavaged with 10^5 CFU of *C difficile* spores. On days 1, 2, and 3 mice were orally gavaged with glycerol trivalerate (n=5) or PBS (n=5). **(B)** *C difficile* TVC were quantified from mouse faecal pellets on days 1, 2, 3, and 4. The box excludes the upper and lower 25% (quartiles) of data,

and the lines go to maximum and minimum values. All data points are marked with “o” in the plot.

Independent t-test of $\log_{10}$-transformed *C difficile* TVC, *p<0.05, ** *p*<0.01.

ACCEPTED MANUSCRIPT

ACCEPTED MANUSCRIPT

TABLES:

Table 1: Time periods used for CDI chemostat experiments to compare the effects of FMT to saline.

Vessel	Days 0-17	Days 18-24	Day 24	Days 25-31	Days 32-42	Day 42	Days 43-54
Control vessel (VA)	Stabilisation period (no intervention)	Stable communities (no intervention)	Added *C difficile* spores	Added *C difficile* spores (day 25) and clindamycin every 12 hrs (days 25-31)	Stabilisation period (no intervention)	**Added saline**	No intervention
Test vessel (VB)	Stabilisation period (no intervention)	Stable communities (no intervention)	Added *C difficile* spores	Added *C difficile* spores (day 25) and clindamycin every 12 hrs (days 25-31)	Stabilisation period (no intervention)	**Added FMT**	No intervention

ACCEPTED MANUSCRIPT

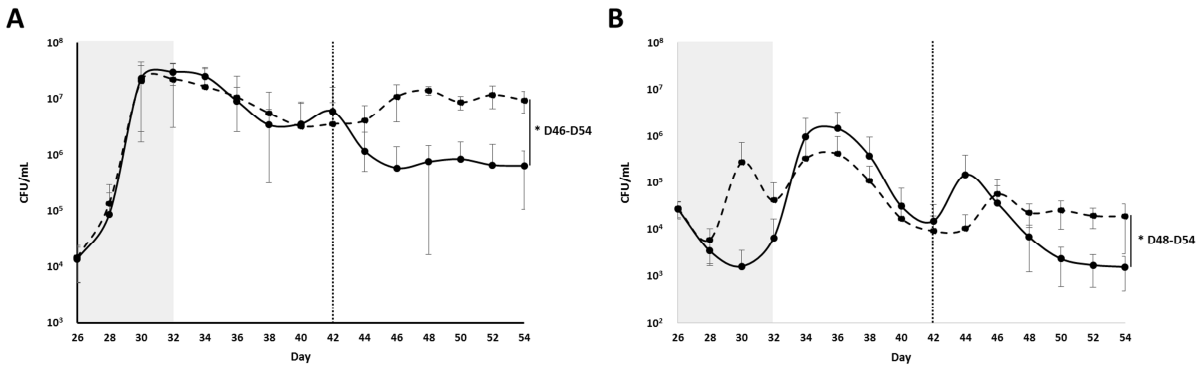

ACCEPTED MANUSCRIPT

ACCEPTED MANUSCRIPT

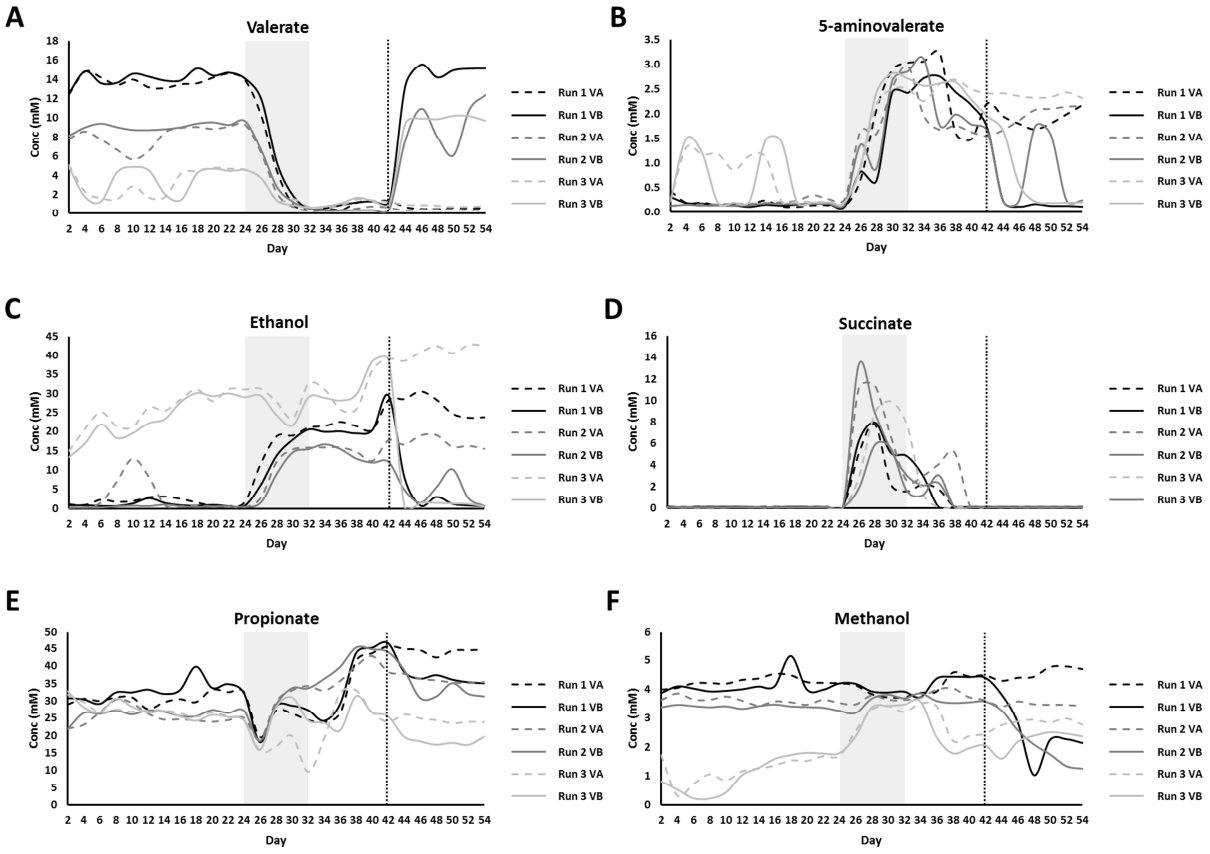

ACCEPTED MANUSCRIPT

ACCEPTED MANUSCRIPT

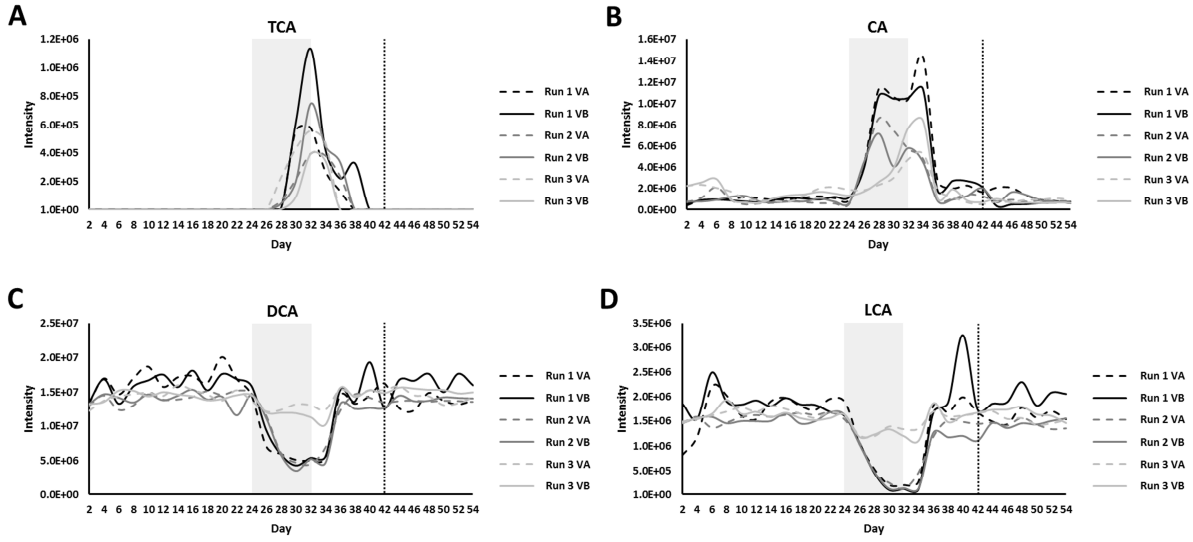

ACCEPTED MANUSCRIPT

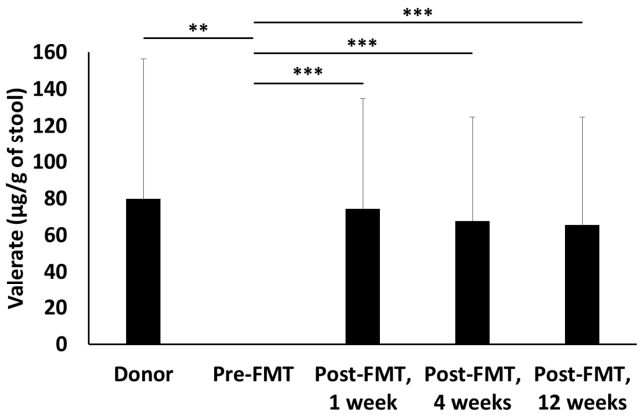

ACCEPTED MANUSCRIPT

ACCEPTED MANUSCRIPT

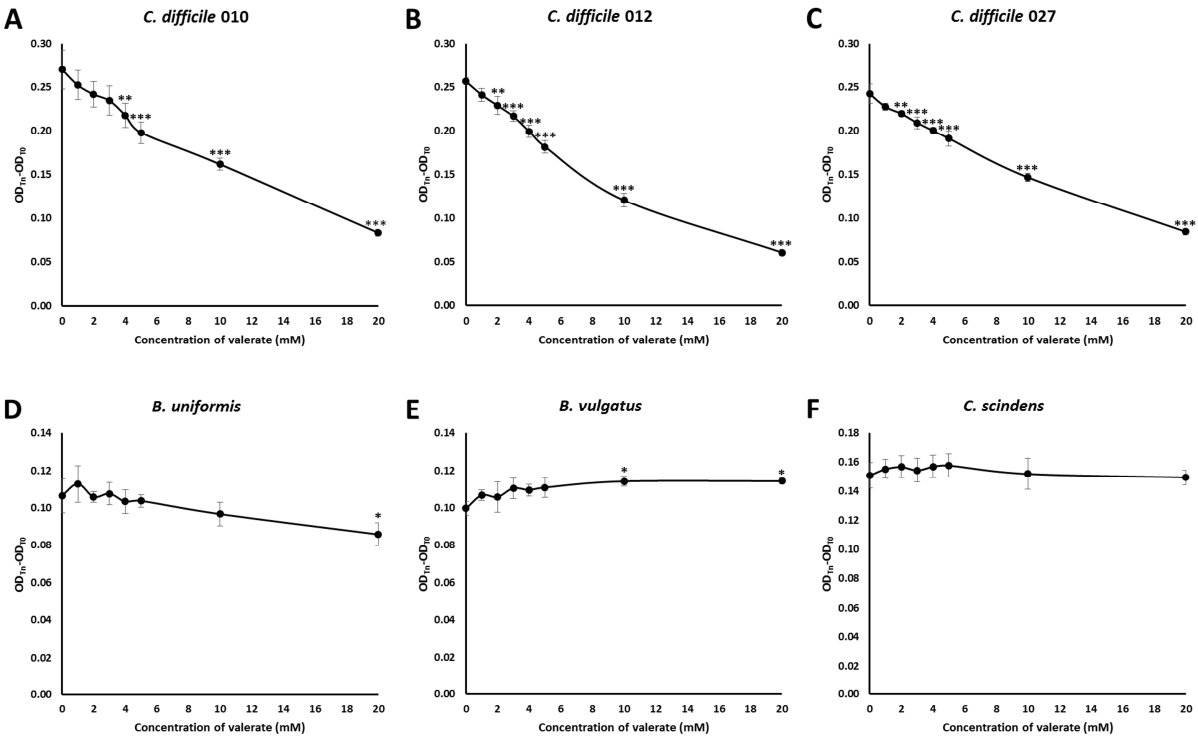

ACCEPTED MANUSCRIPT

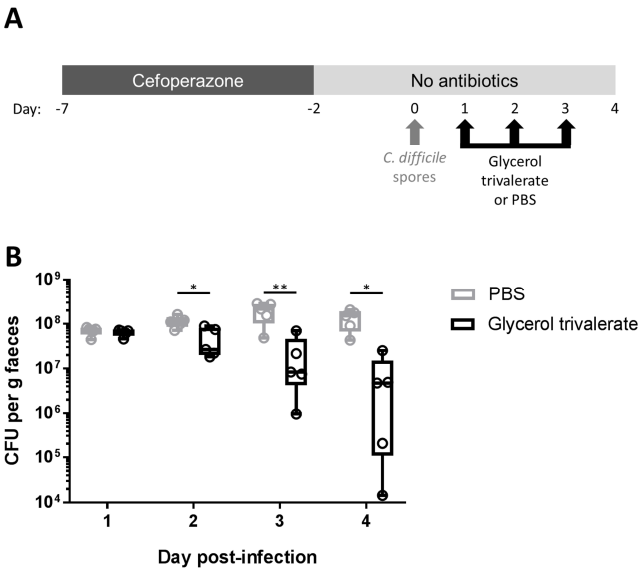

ACCEPTED MANUSCRIPT

ACCEPTED MANUSCRIPT

SUPPLEMENTARY MATERIAL

SUPPLEMENTARY METHODS:

Bacterial strains:

C difficile DS1684 (ribotype 010, non-toxigenic strain) was used for chemostat experiments and mouse experiments. *C difficile* DS1684, *C difficile* CD630 (ribotype 012, virulent multidrug resistant strain), *C difficile* R20291 (ribotype 027, a hypervirulent strain), *Bacteroides uniformis*, *Bacteroides vulgatus*, and *Clostridium scindens* (DSM 5676) were used in batch culture experiments. *C difficile* ribotype 027 is a common ribotype in Europe and North America,[1-3] while ribotype 012 is one of the common ribotypes in mainland China.[4,5] CD630 and R20291 are genetically and phenotypically well-characterised and are good representatives of their ribotypes.[6] *B uniformis* and *B vulgatus* were isolated from the stool of a healthy male in his 30's using fastidious anaerobe agar (Lab M, Heywood, UK) or nutrient agar (Sigma-Aldrich, St. Louis, USA), respectively.

Chemostat model of CDI:

The working volume of each vessel was 235 ml and the growth medium feed was set to a retention time of 21 hours.[7,8] The composition of the growth medium consisted of a mixture of both soluble and insoluble starches, amino acids, peptides, proteins, vitamins, trace elements, and porcine gastric mucin (type II).[9] To mimic the gut environment cultures were maintained at a temperature of 37°C and a pH of 6.8, were gently agitated, and kept anaerobic by sparging with oxygen-free nitrogen gas. Chemostat cultures were sampled daily from each vessel and vessels were operated for 54 days post-inoculation. Chemostat culture samples were aliquoted and stored at -80°C for DNA extraction and mass spectrometry analysis. For NMR analysis, fresh chemostat culture was centrifuged at 20,000 x g and 4°C for 10 minutes, and the supernatant was aliquoted and stored at -80°C.

Design of chemostat experiments:

We induced CDI in our chemostat gut model following a modified version of the methods previously described by Freeman and colleagues (**Table 1**).[10] Briefly, chemostat cultures were grown for 24 days without experimental manipulation to allow the communities to stabilise. After sampling vessels on day 24 we added $7.8x10^6$ *C difficile* spores to each vessel to achieve an initial concentration of $3.3x10^4$ spores/mL.[11] On day 25 we added another dose of $7.8x10^6$ *C difficile* spores to both vessels, and clindamycin was added to both vessels at a final concentration of 33.9 mg/L every 12 hours for 7 days (from days 25-31). After stopping clindamycin dosing chemostat cultures were left to grow for 10 days without experimental manipulation (days 32-42). This was done to allow the perturbed microbial communities to stabilise, so we could more easily determine which bacteria or metabolites were altered by FMT, and which bacteria or metabolites were able to recover after antibiotic treatment in the absence of FMT. After sampling on day 42 we added a single dose of saline to VA (control vessel) and a single dose of FMT to VB (test vessel). Chemostat cultures were then left to grow for a further 12 days without further experimental manipulation to monitor the effects of FMT on the chemostat communities (days 43-54).

***C difficile* spore preparation:**

C difficile spores were prepared using previously described methods.[11] *C difficile* DS1684 was grown anaerobically on fastidious agar plates supplemented with 5% defibrinated horse blood (VWR, Radnor, USA) and incubated at 37°C for 7 days. The growth was removed from the plates using a sterile loop and resuspended in 1 mL sterile water. Next, 1 mL of 95% ethanol was mixed with the cell suspension and was incubated for 1 hour at room temperature. The cell suspension was then centrifuged at 3000 x g and resuspended in 1 mL sterile water. Spores were enumerated by preparing serial 10-fold dilutions in phosphate buffered saline (PBS) (Sigma-Aldrich) and plating the dilutions on Braziers Cycloserine,

Cefoxitin Egg Yolk agar plates (containing Braziers CCEY agar base (Lab M), 250 mg/L cycloserine (VWR), 8 mg/L cefoxitin (Sigma-Aldrich), 8% egg yolk emulsion (SLS, Nottingham UK), 2% lysed defibrinated horse blood (VWR), and 5 mg/L lysozyme (Sigma-Aldrich)).[12] Plates were incubated anaerobically at 37°C for 48 hours and the number of colonies were enumerated.

Enumeration of *C difficile* counts from chemostat culture samples:

C difficile total viable counts and spore counts were quantified from fresh chemostat culture samples every other day starting 26 days post-inoculation. *C difficile* total viable counts (TVC) were enumerated from fresh chemostat culture samples by performing serial 10-fold dilutions in PBS and plating onto Brazier's Cycloserine, Cefoxitin Egg Yolk agar plates (as described above, with the addition of 2 mg/L moxifloxacin (VWR)) in triplicate using the Miles and Misra method.[13] *C difficile* spore counts were enumerated from alcohol-shocked chemostat culture samples by mixing an equal volume of fresh chemostat culture sample with 95% ethanol and incubating at room temperature for one hour. Samples were then centrifuged at 3000 x g and 4°C for 10 minutes and resuspended in PBS. Spores were then quantified by performing serial 10-fold dilutions in PBS and plating onto Brazier's Cycloserine, Cefoxitin Egg Yolk agar plates (as described above, without the addition of moxifloxacin) in triplicate using the Miles and Misra method. Plates were incubated anaerobically at 37°C for two days and colonies were enumerated.

Preparation and instillation of FMT:

Fresh faecal samples were placed into an anaerobic chamber within 5 minutes of defecation. FMT preparations were prepared by homogenising 10 g of stool in 100 mL of anaerobic 0.9% saline in a strainer stomacher bag (250 rpm for 1 min). We added 50 mL of anaerobic saline to VA (control vessel) and 50 mL of homogenised stool to VB (test vessel). For Run 1 and Run 2 the stool transplant was

prepared from the stool of a healthy male donor in his 30's, and for Run 3 the stool transplant was prepared from the stool of a healthy female donor in her 20's. Both individuals have been used as FMT donors to treat CDI patients in Imperial's FMT Programme (and therefore undergone the appropriate donor screening protocols), and had not taken antibiotics for at least 3 months prior to providing the stool sample.

DNA extraction:

DNA was extracted from 250 µL of chemostat culture using the PowerLyzer PowerSoil DNA Isolation Kit (Mo Bio, Carlsbad, USA) following the manufacturer's protocol, except that samples were lysed by bead beating for 3 min at speed 8 using a Bullet Blender Storm instrument (Chembio Ltd, St. Albans, UK). DNA was aliquoted and stored at -80°C until it was ready to be used.

16S rRNA gene qPCR:

16S rRNA gene qPCR data was used to determine the total bacterial biomass within each sample and was performed using extracted chemostat culture DNA to following a previously published protocol.[14] A total volume of 20 µL was used for each reaction and consisted of the following: 1x Platinum Supermix with ROX (Life Technologies, Carlsbad, USA), 1.8 µM BactQUANT forward primer (5'-CCTACGGGAGGCAGCA-3'), 1.8 µM BactQUANT reverse primer (5'-GGACTACCGGGTATCTAATC-3'), 225 nM probe ((6FAM) 5'-CAGCAGCCGCGGTA-3' (MGBNFQ)), PCR grade water (Roche, Penzberg, Germany), and 5 µL DNA. Each PCR plate included a standard curve using *E. coli* DNA (Sigma-Aldrich) (3-300,000 copies per reaction in 10-fold serial dilutions) as well as no template negative controls. All samples, standards, and controls were amplified in triplicate. Extracted DNA samples were diluted to ensure they fell within the standard curve. Amplification and real-time fluorescence detections were performed using the Applied Biosystems StepOnePlus Real-Time PCR System using the following PCR cycling

conditions: 50 °C for 3 min, 95 °C for 10 min, and 40 cycles of 95 °C for 15 sec and 60 °C for 1 min. We used a paired t-test to compare changes in log-transformed 16S rRNA gene copy number between samples at specific time points.

Pre-processing and analysis of 16S rRNA gene sequencing data:

We used the Mothur package (v1.35.1) to preprocess and analyse the resulting sequencing data following the MiSeq SOP Pipeline.[15] We used the Silva bacterial database for sequence alignments (www.arb-silva.de/) and the RDP database reference sequence files for classification of sequences using the Wang method.[16] We determined the Operational Taxonomic Unit (OTU) taxonomies (phylum to genus) using the RDP MultiClassifier script. We resampled and normalised data to the lowest read count in Mothur (9527 reads per sample), which resulted in greater than 99.4% coverage within each sample. We used 16S rRNA gene qPCR data and the following formula to express our 16S rRNA gene sequencing data as absolute abundances (instead of relative abundances):

$$Absolute\ abundance\ of\ taxa = relative\ abundance\ of\ taxa \times \left(\frac{16S\ rRNA\ gene\ copy\ number\ in\ sample}{highest\ 16S\ rRNA\ gene\ copy\ number\ in\ sample\ set}\right)$$

The Shannon diversity index (H'), Pielou evenness index (J'), and richness (total number of bacterial taxa observed, S_{obs}) were calculated using the vegan library[17] within the R statistical package.[18]

Stream plots were prepared by plotting the absolute abundance of 16S rRNA gene sequencing data (biomass-corrected) over time (OTU-level, coloured by phylum). This was accomplished using the streamgraph function within the streamgraph library (v0.8.1) within R.[19]

^{1}H-NMR spectroscopy sample preparation:

Chemostat culture supernatants were randomized and defrosted at room temperature for 1 hour. Once samples were defrosted supernatants were centrifuged at 20,000 x g and 4°C for 10 minutes. Next,

400 µL of chemostat culture supernatant was mixed with 250 µL of sodium phosphate buffer solution (28.85 g Na_2HPO_4 (Sigma-Aldrich), 5.25 g NaH_2PO_4 (Sigma-Aldrich), 1 mM TSP (Sigma-Aldrich), 3 mM NaN_3 (Sigma-Aldrich), deuterium oxide (Goss Scientific Instruments, Crewe, UK) to 1 L, pH 7.4)[20] and 600 µL was pipetted into a 5 mm NMR tube.

Confirmation of NMR metabolite identities using 1D-NMR with spike-in and 2D-NMR spectroscopy:

We used the statistical total correlation spectroscopy (STOCSY) analysis method to aid in the identification of metabolites in NMR spectra by determining correlations between intensities of the various peaks across the whole sample.[21] To further confirm if the peaks assigned to valerate and other metabolites were correct, we also conducted a two-dimensional NMR spectra (including ^1H–^1H TOCSY and ^1H–^1H COSY) for the chemostat culture supernatant and valerate standard using typical parameters to confirm the connectivity of the proton in the metabolites.[22,23]

For the valerate spike-in experiment one-dimensional ^1H NMR spectra were acquired as described in the ^1H-NMR spectroscopy methods section from the main text, except 64 scans were recorded into 65536 data points with a spectral width of 20 ppm. After normal 1D ^1H NOESY NMR acquisition, 10 µL of valerate standard (99%, 0.9 M in PBS buffer) (Fisher Scientific, Hampton, USA) was added into the sample. A one-dimensional spectrum was recorded again to see if the relevant peaks of valerate increased.

Data pre-processing and analysis of UPLC-MS bile acid data:

Quality control samples were prepared using a mixture of equal parts of the chemostat culture supernatants. We used the quality control samples as an assay performance monitor and to guide the removal of features with high variation.[24] We also spiked quality control samples with defined mixtures of bile acids to determine the chromatographic retention times of specific bile acids and to aid in

metabolite identification (55 bile acid standards, including 36 non-conjugated bile acids, 12 tauro-conjugated bile acids, and 7 glyco-conjugated bile acids) (Steraloids, Newport, USA).

We converted the Waters raw data files to NetCDF format and extracted the data using XCMS (v1.50) package implemented within the R (v3.3.1) software. Dilution effects were corrected for using probabilistic quotient normalisation[25] and chromatographic features with high coefficient of variation (higher than 30% in the quality control samples) were excluded from further analysis.

Short AsyNchronous Time-series Analysis (SANTA):

SANTA is an automated pipeline that is implemented within R and controlled through a graphical user interface developed with Shiny. [26,27] This method analyses short time series by estimating trajectories as a smooth spline, and calculates whether time trajectories are significantly altered between different groups or over different time periods. SANTA was used to make the following comparisons: stabilisation period vs. clindamycin-dosing period, stabilisation period vs. post-clindamycin stabilisation period, and FMT-treated vs. saline-treated cultures during the treatment period. We used mean subtraction to eliminate between-run differences in metabolite concentrations that arose from differences in the stool used to seed the chemostat vessels. For each metabolite, we calculated the mean for all samples within the same chemostat run, then we subtracted the mean from all its values within the run.[28] Depending upon the time series being analysed, the number of degrees of freedom (df) to fit the spline model was chosen to avoid overfitting the data (df = 3-5). We report the p_{Dist} values, which uses the area between the mean group fitted curves to determine whether there is a difference between the two groups over time. Analysis used 1000 permutation rounds to calculate p-values and 1000 bootstrap rounds to calculate the 95% confidence bands. Reported p_{Dist} values are with Benjamini-Hochberg FDR correction, and $p < 0.05$ was considered significant.

Integration of 16S rRNA gene sequencing data and metabolite data:

We used regularised Canonical Correlation Analysis (rCCA) to correlate 16S rRNA gene sequencing data (genus level) with bile acid mass spectrometry or ^{1}H-NMR data from the same set of samples using the mixOmics library within R.[29] rCCA is an unsupervised method that maximises the correlation between the two data sets X and Y (information on the treatment groups is not taken into account in the analysis). We used the shrinkage method to determine the regularisation parameters. The plotIndiv function was used to generate unit representation plots, where each point on the scatter plot represents a single chemostat culture sample, and samples were projected into the XY-variate space. The plotVar function was used to generate correlation circle plots, where strong correlations between variables (correlations greater than 0.5) are plotted outside of the inner circle. Variables are represented through their projections onto the planes defined by their respective canonical variates. In this plot the variables projected in the same direction from the origin have a strong positive correlation, and variables projected in opposite directions form the origin have strong negative correlations. Variables with stronger correlations sit at farther distances from the origin.

***C difficile* germination batch cultures with taurocholic acid (TCA):**

To test the effects of TCA on *C difficile* germination we resuspended *C difficile* DS1684 spores in supplemented brain heart infusion broth with or without 1% TCA (Sigma-Aldrich) in triplicate.[30] The OD_{600} was measured immediately after inoculation of broths (time zero) and after an overnight incubation at 37°C in anaerobic chamber. A paired t-test was used to determine whether TCA affected *C difficile* germination.

***C difficile* vegetative growth batch cultures with TCA:**

To test the effects of TCA on *C difficile* vegetative growth we centrifuged an overnight culture of *C difficile* DS1684 at 3000 x g for 10 minutes and resuspended the cells in supplemented brain heart infusion broth with or without 1% TCA (in triplicate). The OD_{600} was measured at time zero and cultures were incubated at 37°C in an anaerobic chamber. Additional OD_{600} measurements were taken at 2, 4, 6, and 8 hours post-inoculation, and the change in OD_{600} was plotted against time. A paired t-test was used to determine whether TCA affected vegetative growth during the exponential phase.

SUPPLEMENTARY RESULTS:

***C difficile* total viable counts and spore counts:**

There was no significant difference in *C difficile* TVC at the end of the clindamycin-dosing period compared to TVC immediately prior to administering FMT or saline treatment ($p>0.05$). There was also no significant difference in *C difficile* TVC in vessels assigned to receive FMT or saline treatment immediately prior to administering the treatment ($p>0.05$).

^{1}H-NMR spectroscopy:

Following FMT or saline treatment there were significant strong negative correlations between valerate and 5-aminovalerate (r_S=-0.76, p=5.27x10^{-6}), ethanol (r_S=-0.69, p=6.53x10^{-5}), and methanol (r_S=-0.78, p=3.11x10^{-6}).

Confirmation of valerate in chemostat culture supernatant by 1D- and 2D-NMR:

The chemical shifts for the 1D ^{1}H-NMR spectrum of 99% valerate standard were: 0.9 (t), 1.3 (dt), 1.46 (m), 2.2 (t) (**Figure S5A**). Overlay of the 1D ^{1}H-NMR spectrum of the valerate standard with the sample showed that each peak of the valerate standard is visible in the sample (**Figure S5B**). Overlay of 1D ^{1}H-NMR spectra of the sample before and after valerate spike-in showed that all the valerate peaks

increased after spike-in (**Figure S5C**). For 2D-NMR analysis overlay of the ^{1}H-^{1}H COSY spectrum of the valerate standard with the sample showed that each peak of the valerate standard was present in the sample spectrum (**Figure S6A**). Overlay of ^{1}H-^{1}H TOCSY spectrum of the valerate standard with the sample showed that each peak of the valerate standard was present in the sample spectrum (**Figure S6B**).

SUPPLEMENTARY DISCUSSION:

Valerate is not expected to be harmful to host gut cells, as exposure of gut organoids to 5 mM valerate did not result in cell death or cause significant alterations in gene expression (Drs. Lee Parry and Richard Brown of the European Cancer Stem Cell Research Institute, personal communication, 19 Dec. 2017). Moreover, mice that received 15 mM glycerol trivalerate in our study did not show any adverse reactions.

The bacterial enzyme 7-α-dehydroxylase is responsible for converting unconjugated primary bile acids CA and CDCA to the secondary bile acids DCA and LCA, respectively. DCA and LCA have been shown to inhibit *C difficile* vegetative growth at specific concentrations,[30,31] and a previous study has shown that DCA and LCA were depleted in pre-FMT samples from recurrent CDI patients, but were restored in post-FMT samples.[32] These findings led researchers to propose antibiotic exposure results in the loss of bacteria with 7-α-dehydroxylase activity, reducing DCA and LCA production and permitting *C difficile* vegetative growth. A study by Buffie and colleagues found that administration of *Clostridium scindens* (a bacterium with 7-α-dehydroxylase activity) was associated with resistance to *C difficile* by restoring the production of the secondary bile acids DCA and LCA.[33] However, in our study we found that the levels of DCA and LCA recovered in chemostat cultures following the cessation of clindamycin. While we did find strong negative correlations between *C difficile* TVC and the secondary bile acids DCA and LCA, recovery of these bile acids to pre-clindamycin levels was not enough to decrease vegetative *C*

difficile counts in chemostat cultures. Indeed, while DCA can inhibit *C difficile* vegetative growth, it appears that DCA can also encourage spore germination at specified concentrations.[30] A better strategy to prevent CDI prior to antibiotic exposure would be to prevent germination altogether by degrading TCA, a potent pro-germinant, using bile salt hydrolase enzymes.

Our chemostat experiments more closely modelled the first episode of CDI and not recurrent CDI. In first episodes of CDI, human patients are exposed to *C difficile* spores while taking an inciting antibiotic (e.g. clindamycin). In our study clindamycin exposure was sufficient to deplete valerate and elevate levels of TCA, allowing *C difficile* spore germination and vegetative growth. We waited 10 days after stopping clindamycin dosing before administering the FMT preparation to allow the perturbed microbial communities to stabilise following the cessation of antibiotics. This delay allowed us to more easily determine which metabolites were altered only by FMT, and which metabolites were able to recover after antibiotic treatment (in the absence of FMT). This feature is a major advantage of performing chemostat studies, as it would be unethical to withhold treatment from recurrent CDI patients in human studies to determine which metabolites would recover in the absence of FMT. We found no significant difference in *C difficile* TVC at the end of the clindamycin-dosing period compared to TVC immediately prior to administering FMT or saline treatment (see Supplementary Results). This means the metabolites that recovered following the cessation of clindamycin dosing, but before FMT, did not affect the vegetative growth of *C difficile* (i.e. bile acids). However, we did see a significant decrease in *C difficile* TVC and spore counts after FMT. This decrease suggests that bacterial metabolites that decreased *C difficile* counts did not recover after stopping clindamycin, but only recovered with FMT (i.e. valerate).

Most human studies of CDI have focused on recurrent CDI, not first episode of CDI. In this study we showed that valerate was depleted in recurrent CDI patients pre-FMT, but was restored post-FMT. To our knowledge this is the first study to measure valerate in the stool of recurrent CDI patients pre- and post-FMT. A previous study by Weingarden and colleagues found that TCA was elevated in the stool of

recurrent CDI patients pre-FMT, but was decreased post-FMT.[32] It is important to note that in these human studies recurrent CDI patients were taking vancomycin when pre-FMT samples were collected, and FMT was administered to recurrent CDI patients within 1-2 days of stopping vancomycin therapy. While we could have designed our chemostat experiments to also include a vancomycin dosing regimen, followed by FMT administration 1-2 days later, broad-spectrum vancomycin therapy would have killed more gut bacteria and depleted the chemostat cultures of additional ecosystem functions that were not important for the establishment of the infection, leading to false positives once these functionalities were restored following FMT. In our chemostat experiments FMT was administered 10 days after stopping clindamycin and pre-FMT samples were collected immediately prior to FMT administration. Had we chosen to administer the FMT preparation within 1-2 days after stopping clindamycin we would expect TCA levels to decrease with FMT.

REFERENCES:

1. Wilcox MH, Shetty N, Fawley WN, *et al*. Changing epidemiology of *Clostridium difficile* infection following the introduction of a national ribotyping-based surveillance scheme in England. Clin Infect Dis 2012;55:1056-1063.
2. Waslawski S, Lo ES, Ewing SA, *et al*. *Clostridium difficile* ribotype diversity at six health care institutions in the United States. J Clin Microbiol 2013;51:1938-1941.
3. Davies KA, Longshaw CM, Davis GL, *et al*. Underdiagnosis of *Clostridium difficile* across Europe: the European, multicentre, prospective, biannual, point-prevalence study of *Clostridium difficile* infection in hospitalised patients with diarrhoea (EUCLID). Lancet Infect Dis 2014;14:1208-1219.
4. Huang H, Fang H, Weintraub A, *et al*. Distinct ribotypes and rates of antimicrobial drug resistance in *Clostridium difficile* from Shanghai and Stockholm. Clin Microbiol Infect 2009;15:1170-1173.

5. Hawkey PM, Marriott C, Liu WE, *et al*. Molecular epidemiology of *Clostridium difficile* infection in a major Chinese hospital: an underrecognized problem in Asia? J Clin Microbiol 2013;51:3308-3313.

6. Dawson LF, Valiente E, Donahue EH, *et al*. Hypervirulent *Clostridium difficile* PCR-ribotypes exhibit resistance to widely used disinfectants. PLoS One 2011;6:e25754.

7. Allison C, McFarlan C, MacFarlane GT. Studies on mixed populations of human intestinal bacteria grown in single-stage and multistage continuous culture systems. Appl Environ Microbiol 1989;55:672-678.

8. Duncan SH, Scott KP, Ramsay AG, *et al*. Effects of alternative dietary substrates on competition between human colonic bacteria in an anaerobic fermentor system. Appl Environ Microbiol 2003;69:1136-1142.

9. McDonald JA, Schroeter K, Fuentes S, *et al*. Evaluation of microbial community reproducibility, stability and composition in a human distal gut chemostat model. J Microbiol Methods 2013;95:167-174.

10. Freeman J, Baines SD, Saxton K, *et al*. Effect of metronidazole on growth and toxin production by epidemic *Clostridium difficile* PCR ribotypes 001 and 027 in a human gut model. J Antimicrob Chemother 2007;60:83-91.

11. Freeman J, O'Neill FJ, Wilcox MH. Effects of cefotaxime and desacetylcefotaxime upon *Clostridium difficile* proliferation and toxin production in a triple-stage chemostat model of the human gut. J Antimicrob Chemother 2003;52:96-102.

12. Crowther GS, Chilton CH, Todhunter SL, *et al*. Comparison of planktonic and biofilm-associated communities of *Clostridium difficile* and indigenous gut microbiota in a triple-stage chemostat gut model. J Antimicrob Chemother 2014;69:2137-2147.

13. Miles AA, Misra SS, Irwin JO. The estimation of the bactericidal power of the blood. J Hyg (Lond) 1938;38:732-749.

14. Liu CM, Aziz M, Kachur S, *et al*. BactQuant: an enhanced broad-coverage bacterial quantitative real-time PCR assay. BMC Microbiol 2012;12:56-2180-12-56.

15. Kozich JJ, Westcott SL, Baxter NT, *et al*. Development of a dual-index sequencing strategy and curation pipeline for analyzing amplicon sequence data on the MiSeq Illumina sequencing platform. Appl Environ Microbiol 2013;79:5112-5120.

16. Wang Q, Garrity GM, Tiedje JM, *et al*. Naive Bayesian classifier for rapid assignment of rRNA sequences into the new bacterial taxonomy. Appl Environ Microbiol 2007;73:5261-5267.

17. Oksanen J, Blanchet FG, Friendly M, *et al*. vegan: Community Ecology Package. R package version 2.4-3.; 2017. Available at: https://CRAN.R-project.org/package=vegan, 2017.

18. R Core Team. R: A language and environment for statistical computing. R Foundation for Statistical Computing, Vienna, Austria.; 2015. Available at: https://www.R-project.org/, 2017.

19. Rudis B. streamgraph: streamgraph is an htmlwidget for building streamgraph visualizations. R package version 0.8.1.; 2015. Available at: http://github.com/hrbrmstr/streamgraph, 2017.

20. Beckonert O, Keun HC, Ebbels TM, *et al*. Metabolic profiling, metabolomic and metabonomic procedures for NMR spectroscopy of urine, plasma, serum and tissue extracts. Nat Protoc 2007;2:2692-2703.

21. Cloarec O, Dumas ME, Craig A, *et al*. Statistical total correlation spectroscopy: an exploratory approach for latent biomarker identification from metabolic ^{1}H NMR data sets. Anal Chem 2005;77:1282-1289.

22. Liu Z, Wang L, Zhang L, *et al*. Metabolic Characteristics of 16HBE and A549 Cells Exposed to Different Surface Modified Gold Nanorods. Adv Healthc Mater 2016;5:2363-2375.

23. Dai H, Xiao C, Liu H, *et al*. Combined NMR and LC-DAD-MS analysis reveals comprehensive metabonomic variations for three phenotypic cultivars of Salvia Miltiorrhiza Bunge. J Proteome Res 2010;9:1565-1578.

24. Sangster T, Major H, Plumb R, *et al*. A pragmatic and readily implemented quality control strategy for HPLC-MS and GC-MS-based metabonomic analysis. Analyst 2006;131:1075-1078.

25. Veselkov KA, Vingara LK, Masson P, *et al*. Optimized preprocessing of ultra-performance liquid chromatography/mass spectrometry urinary metabolic profiles for improved information recovery. Anal Chem 2011;83:5864-5872.

26. Chang W, Cheng J, Allaire JJ, *et al*. shiny: Web Application Framework for R. R package version 1.0.3.; 2017. Available at: https://CRAN.R-project.org/package=shiny, 2017.

27. Wolfer A. SANTA-App: Interactive package for Short AsyNchronous Time-series Analysis (SANTA) in R, implemented in Shiny; 2017. Available at: https://github.com/adwolfer/SANTA-App, 2017.

28. **Gratton J**, **Phetcharaburanin J**, Mullish BH, *et al*. Optimized Sample Handling Strategy for Metabolic Profiling of Human Feces. Anal Chem 2016;88:4661-4668.

29. Le Cao K, Rohart F, Gonzalez I, *et al*. mixOmics: Omics Data Integration Project. R package version 6.1.2.; 2017. Available at: https://CRAN.R-project.org/package=mixOmics, 2017.

30. Sorg JA, Sonenshein AL. Bile salts and glycine as cogerminants for *Clostridium difficile* spores. J Bacteriol 2008;190:2505-2512.

31. Thanissery R, Winston JA, Theriot CM. Inhibition of spore germination, growth, and toxin activity of clinically relevant *C difficile* strains by gut microbiota derived secondary bile acids. Anaerobe 2017;45:86-100.

32. **Weingarden AR**, **Chen C**, Bobr A, *et al*. Microbiota transplantation restores normal fecal bile acid composition in recurrent *Clostridium difficile* infection. Am J Physiol Gastrointest Liver Physiol 2014;306:G310-9.

33. Buffie CG, Bucci V, Stein RR, *et al*. Precision microbiome reconstitution restores bile acid mediated resistance to *Clostridium difficile*. Nature 2015;517:205-208.

Author names in bold designate shared co-first authorship

SUPPLEMENTARY FIGURE LEGENDS:

Figure S1: Stream plots showing the OTU abundances in each chemostat culture over time. Each stream of colour represents an OTU, and streams are grouped by phylum: *Bacteroidetes* (blue), *Firmicutes* (green), *Proteobacteria* (orange), *Verrucomicrobia* (purple), unclassified (grey), and *C difficile* (red). The width of the stream represents the OTU abundance at each time point. The dotted box indicates the clindamycin-dosing period, while the dotted vertical line indicates the day of FMT or saline dosing.

Figure S2: Diversity of bacterial communities cultured in chemostat vessels (VA= saline-treated cultures, dashed line; VB= FMT-treated cultures, solid line). **(A)** Shannon diversity index (H'), **(B)** Richness (S_{obs}), **(C)** Pielou's evenness index (J'). The shaded grey box indicates the clindamycin-dosing period, while the vertical dotted line indicates the day of FMT or saline dosing. SANTA analysis with Benjamini-Hochberg FDR was used to compare the following: steady state cultures to clindamycin-treated cultures, steady state cultures to post-clindamycin cultures, and FMT-treated cultures to saline treated cultures.

Figure S3: ^{1}H-NMR metabolites that changed following clindamycin treatment and with FMT (VA= saline-treated cultures, dashed line; VB= FMT-treated cultures, solid line). **(A)** butyrate, **(B)** acetate, **(C)** isobutyrate, and **(D)** isovalerate. The shaded grey box indicates the clindamycin-dosing time period, while the vertical dotted line indicates the day of FMT or saline dosing. SANTA analysis with Benjamini-Hochberg FDR was used to compare the following: steady state cultures to clindamycin-treated cultures, steady state cultures to post-clindamycin cultures, and FMT-treated cultures to saline treated cultures.

Figure S4: Regularized CCA (rCCA) model correlating 16S rRNA gene sequencing data (genus-level) and ^{1}H-NMR metabolite data. **(A)** The representation of units (a.k.a. samples) for the first two canonical variates showing the correlations between variables before (grey), during (blue), and after (orange) the clindamycin-dosing period. "A" represents samples collected from VA and "B" represents samples from

VB. **(B)** Correlation circle plot showing strong correlations between variables before, during, and after the clindamycin-dosing period. Metabolites are shown in blue and bacterial genera are shown in orange. *Clostridium* cluster XI (the clostridial cluster that includes *C difficile*) is shown in a black box. **(C)** The representation of units (a.k.a. samples) for the first two canonical variates showing the correlations between variables following FMT (blue) or saline (orange) treatment. "A" represents samples collected from VA (saline-treated cultures) and "B" represents samples from VB (FMT-treated cultures). **(D)** Correlation circle plot showing strong correlations between variables following FMT or saline treatment. Metabolites are shown in blue and bacterial genera are shown in orange. *Clostridium* cluster XI (the clostridial cluster that includes *C difficile*) is shown in a black box.

Figure S5: 1D ^{1}H-NMR to confirm the identity of valerate in chemostat culture supernatants. **(A)** 1D ^{1}H-NMR spectrum of valerate standard (blue). **(B)** Overlay of 1D ^{1}H-NMR spectrum of valerate standard (blue) with sample spectrum (red). Each peak of the valerate standard is visible in the sample spectrum. **(C)** Overlay of 1D ^{1}H-NMR spectra of sample before (blue) and after (red) valerate spike-in. All the peaks proposed to belong to valerate increased following spike in with valerate standard (green).

Figure S6: 2D ^{1}H-NMR to confirm the identity of valerate in chemostat culture supernatants. **(A)** Overlay of the ^{1}H-^{1}H COSY spectrum of valerate standard (blue) with sample spectrum (red). Each peak of the valerate standard is visible in the sample spectrum. **(B)** Overlay of the ^{1}H-^{1}H TOCSY spectrum of valerate standard (blue) with sample spectrum (red). Again, each peak of the valerate standard is visible in the sample spectrum.

Figure S7: Overlay of ^{1}H-^{1}H COSY sample spectrum (blue) and ^{1}H-^{1}H TOCSY sample spectrum (red) to confirm the identity of other metabolites found in chemostat culture supernatants.

Figure S8: Statistical total correlation spectroscopy (STOCSY). **(A)** 5-aminovalerate STOCSY spectrum obtained by correlating all points in the spectra with the 5-aminovalerate resonance at 3.019 ppm. Peak clusters with high correlations (*) correspond to positions where we expected to see peaks for 5-

aminovalerate. **(B)** Succinate STOCSY spectrum obtained by correlating all points in the spectra with the succinate resonance at 2.408 ppm. No other peaks had high correlations with the peak at 2.408, confirming this peak belonged to succinate.

Figure S9: Bile acids that changed following clindamycin treatment (VA= saline-treated cultures, dashed line; VB= FMT-treated cultures, solid line). **(A)** taurodeoxycholic acid (TDCA), **(B)** glycocholic acid (GCA), **(C)** glycodeoxycholic acid (GDCA), **(D)** glycochenodeoxycholic acid (GCDCA), **(E)** chenodeoxycholic acid (CDCA), and **(F)** ursodeoxycholic acid (UDCA). The shaded grey box indicates the clindamycin-dosing period, while the vertical dotted line indicates the day of FMT or saline dosing. Steady state cultures were compared to clindamycin-treated cultures using SANTA analysis with Benjamini-Hochberg FDR.

Figure S10: Regularized CCA (rCCA) model correlating 16S rRNA gene sequencing data (genus-level) and bile acid data. **(A)** The representation of units (a.k.a. samples) for the first two canonical variates showing the correlations between variables before (grey), during (blue), and after (orange) the clindamycin-dosing period. "A" represents samples collected from VA and "B" represents samples from VB. **(B)** Correlation circle plot showing strong correlations between variables before, during, and after the clindamycin-dosing period. Bile acids are shown in blue and bacterial genera are shown in orange. *Clostridium* cluster XI (the clostridial cluster that includes *C difficile*) is shown in a black box.

Figure S11: TCA is required for *C difficile* spore germination, but has no effect on *C difficile* vegetative growth. **(A)** *C difficile* spores were incubated supplemented brain heart infusion broth in the presence and absence of 1% TCA and grown overnight. There was a significant increase in *C difficile* germination in the presence of TCA (*** p<0.001). **(B)** *C difficile* vegetative cells were inoculated into supplemented brain heart infusion broth in the presence and absence of 1% TCA. There were no significant differences in the growth of *C difficile* in the presence or absence of TCA at any time point in the growth curve. Growth of *C difficile* in the broths was quantified by taking OD_{600} measurements using a plate spectrometer. Error bars represent the mean ± standard deviation.

Figure S12: Schematic of key metabolite interactions with *C difficile* during health, CDI, and recurrent CDI. Initial antibiotic treatment decreases the diversity of the gut microbiota, killing bacteria that produce valerate and bile salt hydrolase (an enzyme that degrades TCA). This results in increased levels of TCA and decreased levels of valerate, allowing for *C difficile* spore germination and vegetative growth (respectively). Treatment for CDI (vancomycin/metronidazole) decreases *C difficile* vegetative cells, but *C difficile* spores remain and microbial community diversity remains low. Again, this antibiotic exposure results in an environment with high TCA and low valerate, allowing the remaining *C difficile* spores to germinate and grow once vancomycin/metronidazole is stopped. When a patient receives FMT for recurrent CDI (usually within 1-2 days of stopping suppressive antibiotics) valerate levels (and valerate producing bacteria) and bile salt hydrolase levels (and bile salt hydrolysing bacteria) are restored, resulting in an environment that inhibits both *C difficile* germination and vegetative growth.

ACCEPTED MANUSCRIPT

ACCEPTED MANUSCRIPT

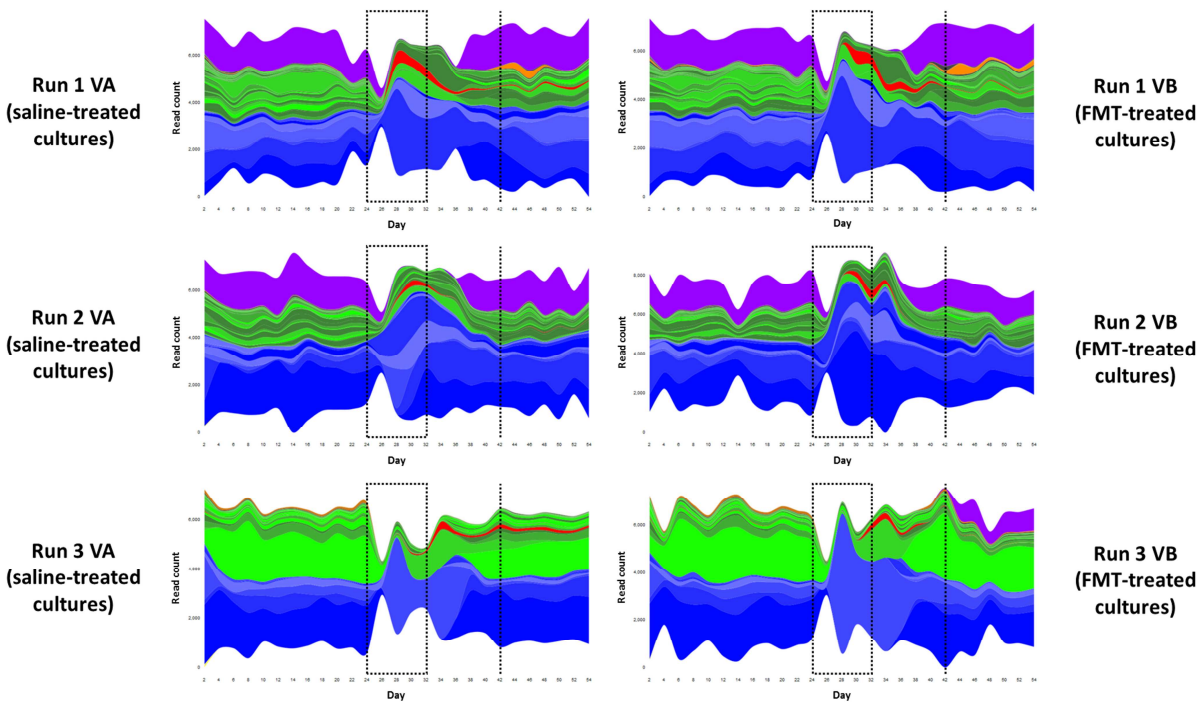

ACCEPTED MANUSCRIPT

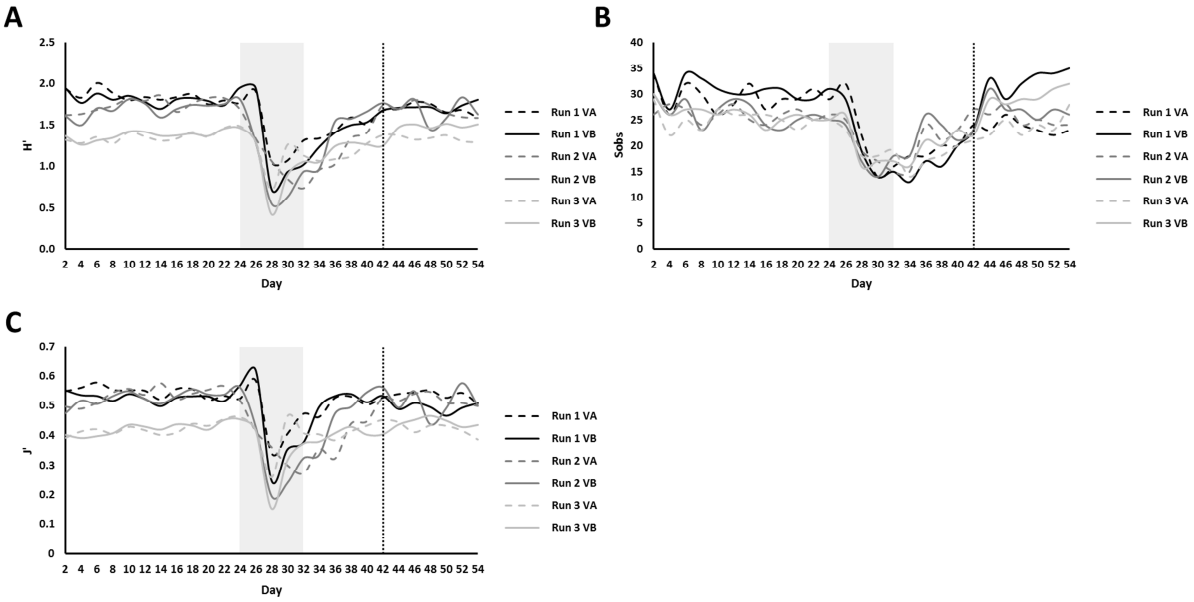

ACCEPTED MANUSCRIPT

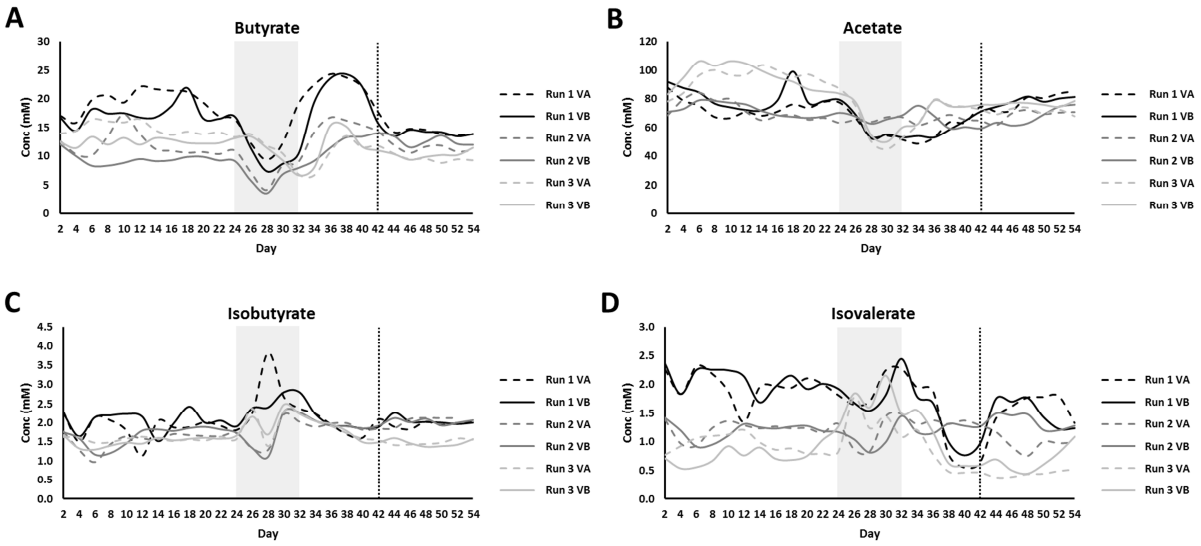

ACCEPTED MANUSCRIPT

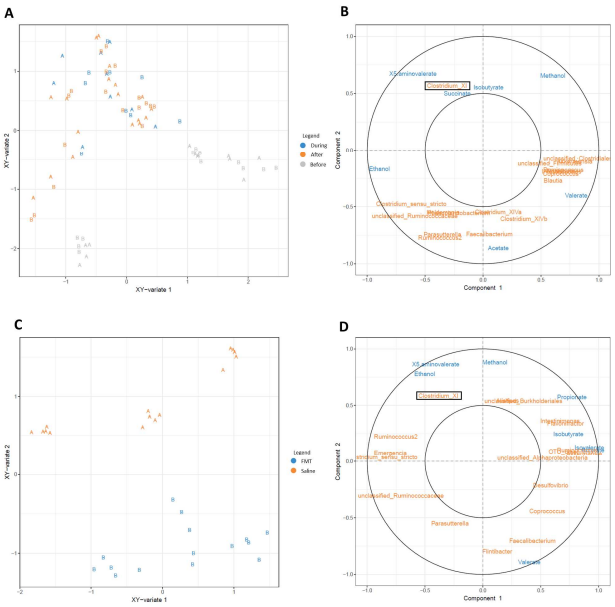

ACCEPTED MANUSCRIPT

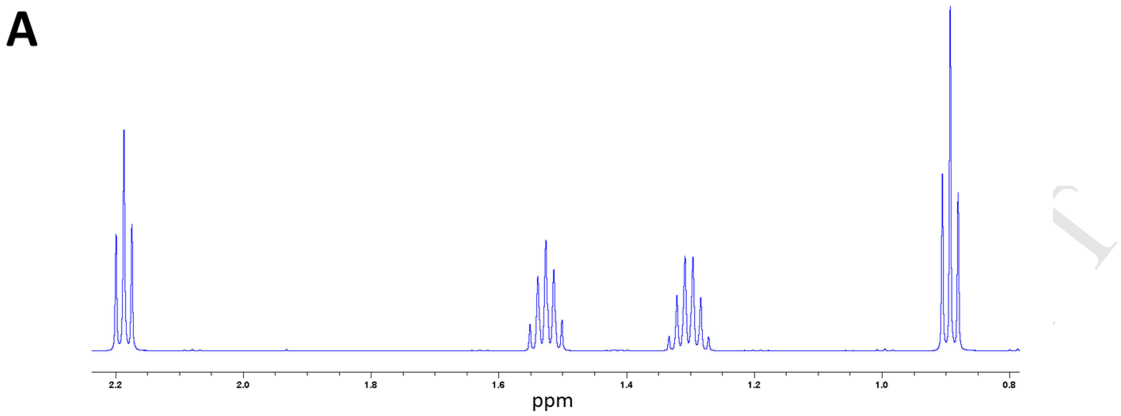
A
2.2
2.0
1.8
1.6
1.4
1.2
1.0
0.8
ppm

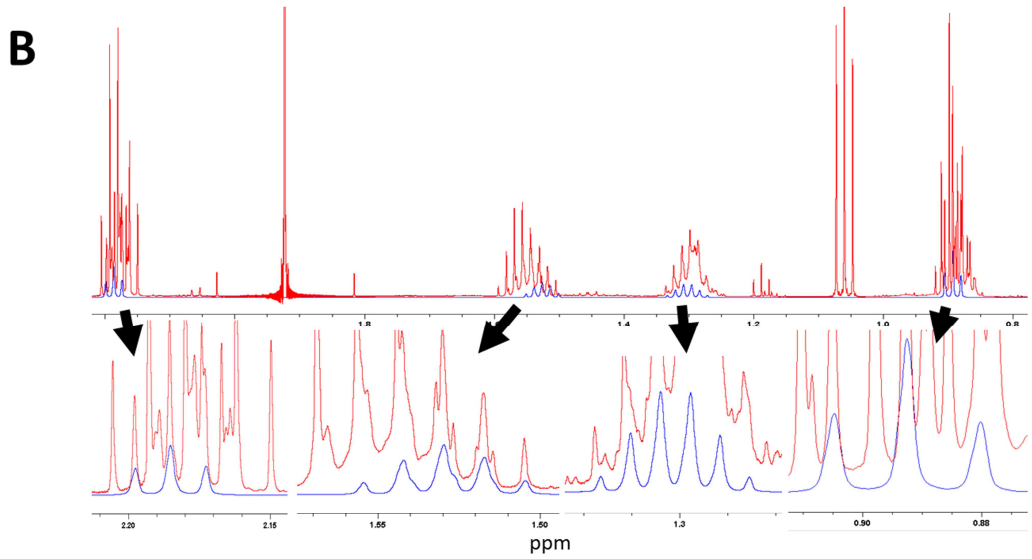
B
2.20
2.15
1.55
1.50
1.3
0.90
0.88
ppm

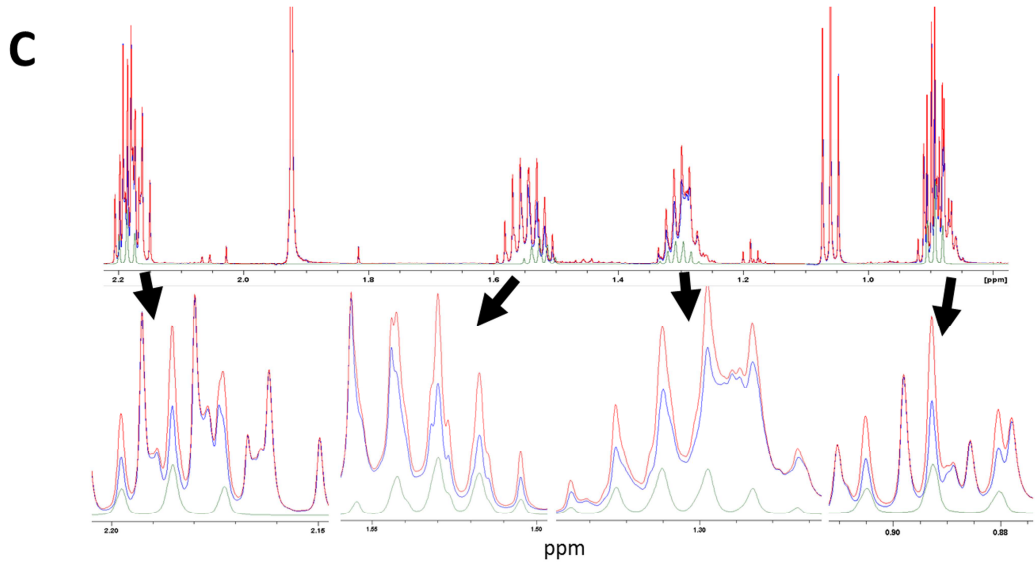
C
2.2
2.0
1.8
1.6
1.4
1.2
1.0
[ppm]
2.20
2.15
1.55
1.50
1.30
0.90
0.88
ppm

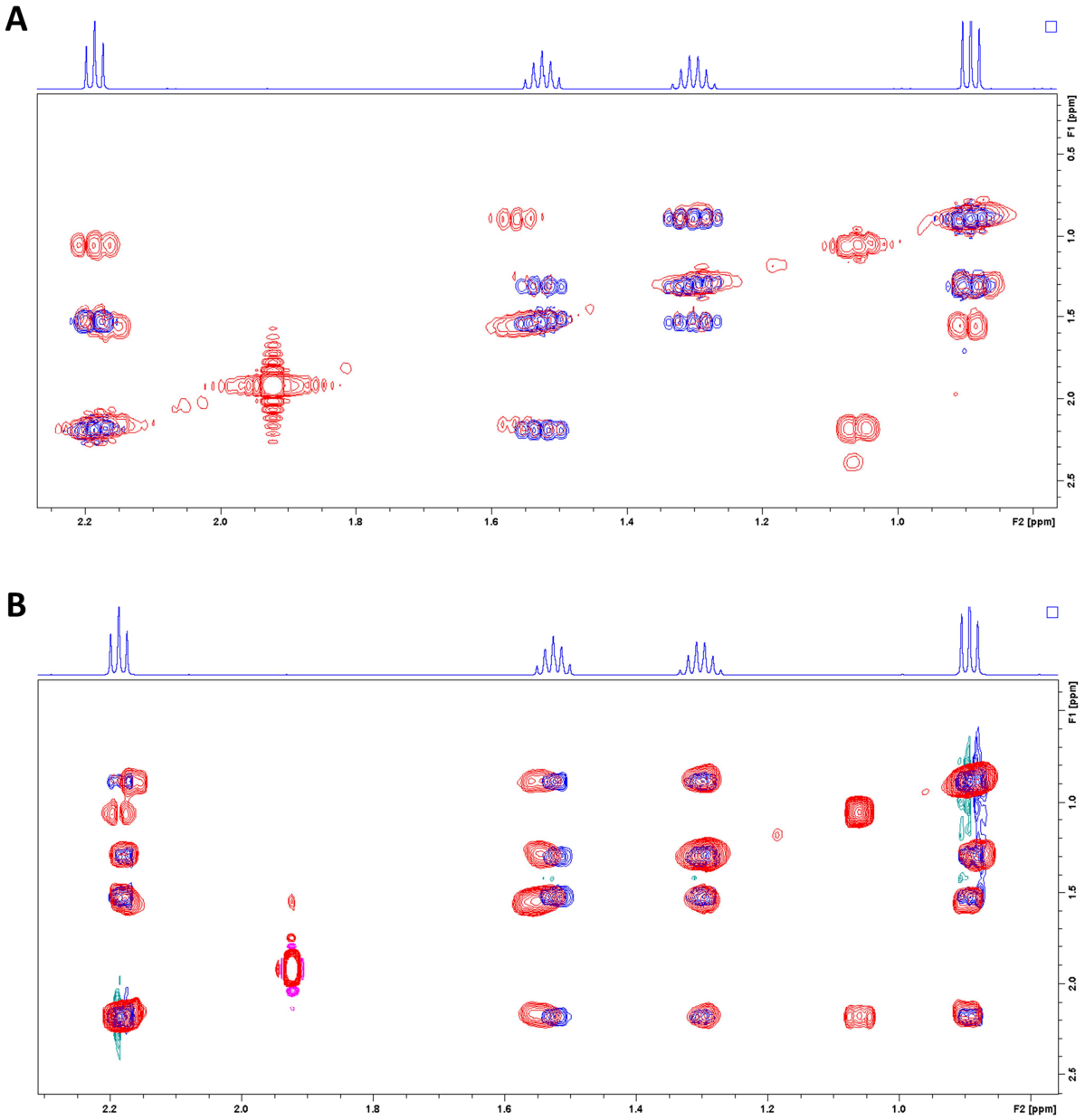
A
F1 [ppm]
0.5
1.0
1.5
2.0
2.5
2.2
2.0
1.8
1.6
1.4
1.2
1.0
F2 [ppm]
B
F1 [ppm]
1.0
1.5
2.0
2.5
2.2
2.0
1.8
1.6
1.4
1.2
1.0
F2 [ppm]

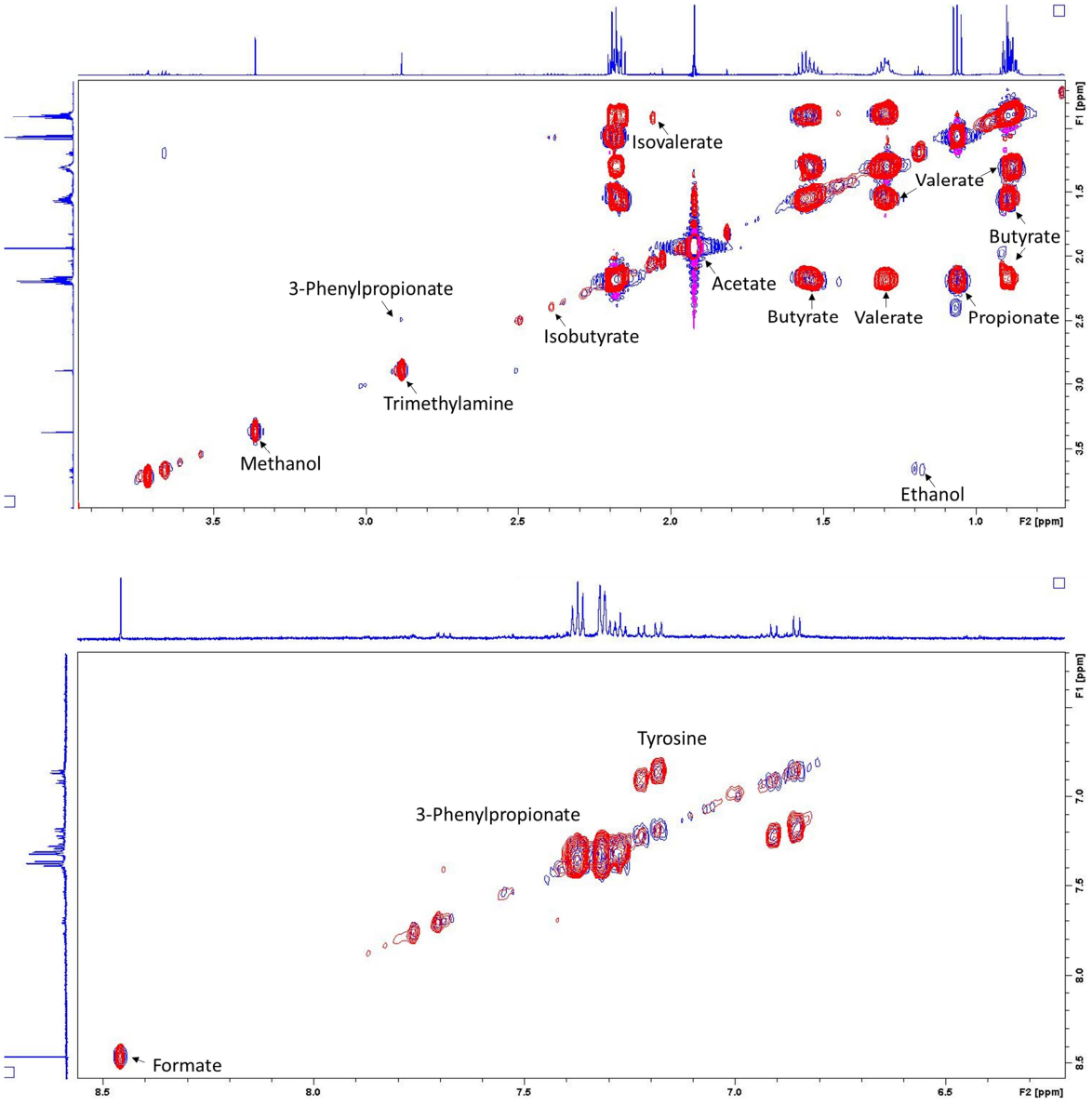
Isovalerate
Valerate
Butyrate
Acetate
3-Phenylpropionate
Isobutyrate
Butyrate
Valerate
Propionate
Trimethylamine
Methanol
Ethanol
F1 [ppm]
F2 [ppm]
Tyrosine
3-Phenylpropionate
Formate
F1 [ppm]
F2 [ppm]

A

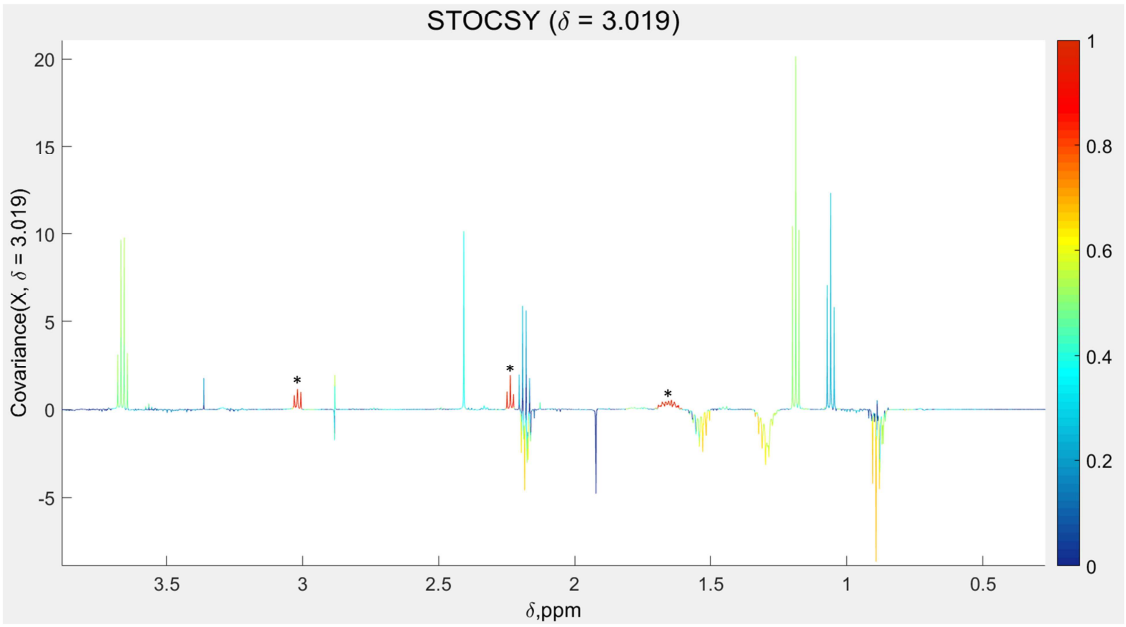
STOCSY (δ = 3.019)
Covariance(X, δ = 3.019)
δ,ppm

B

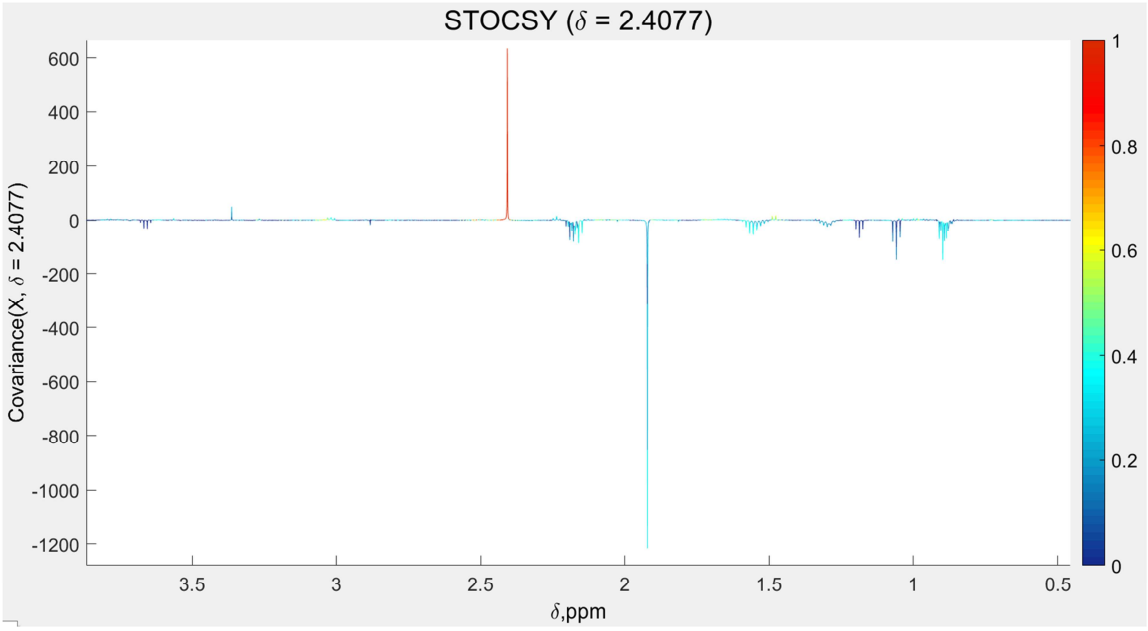
STOCSY (δ = 2.4077)
Covariance(X, δ = 2.4077)
δ,ppm

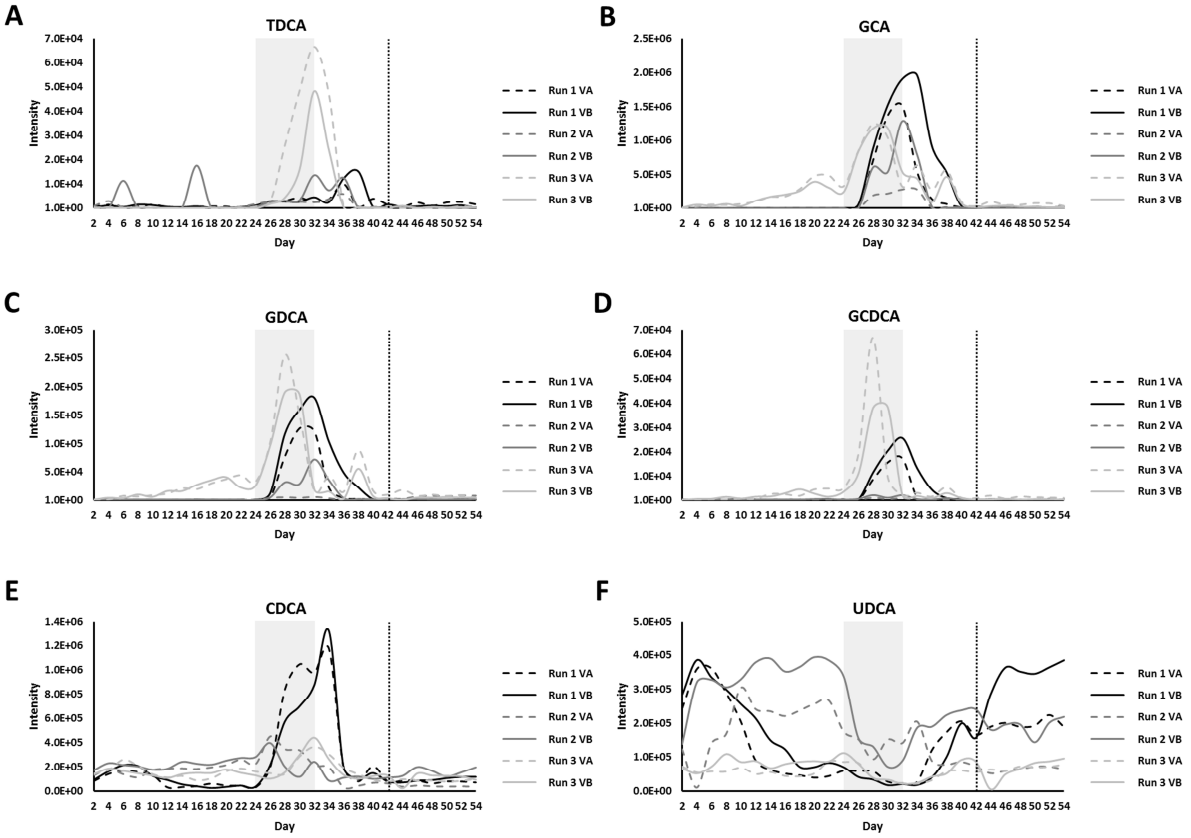

ACCEPTED MANUSCRIPT

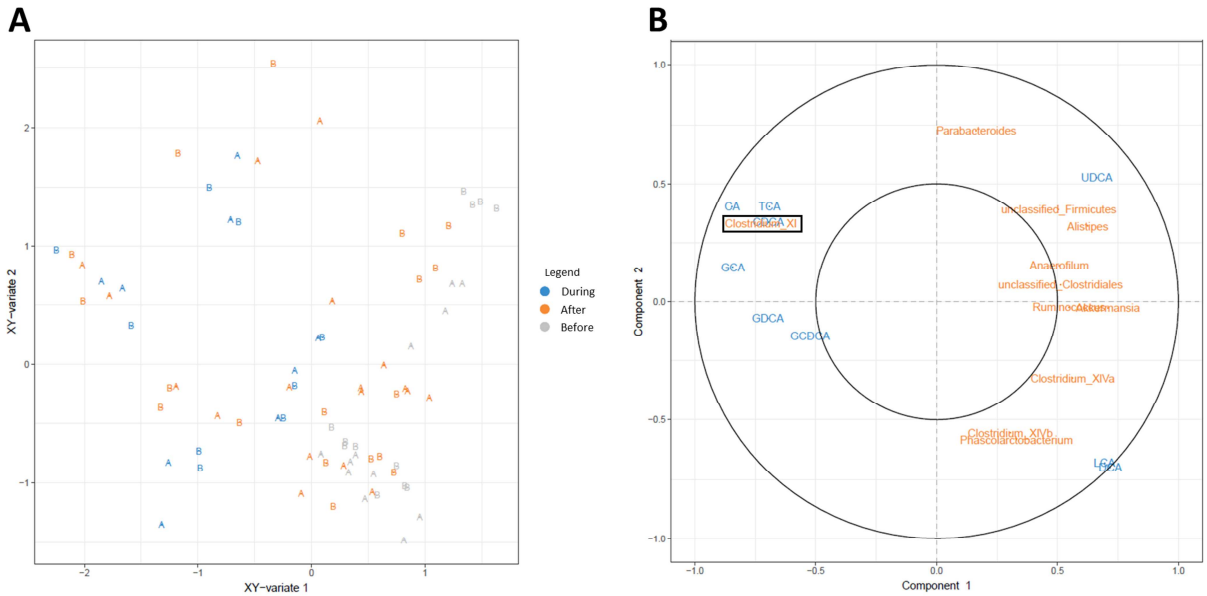

ACCEPTED MANUSCRIPT

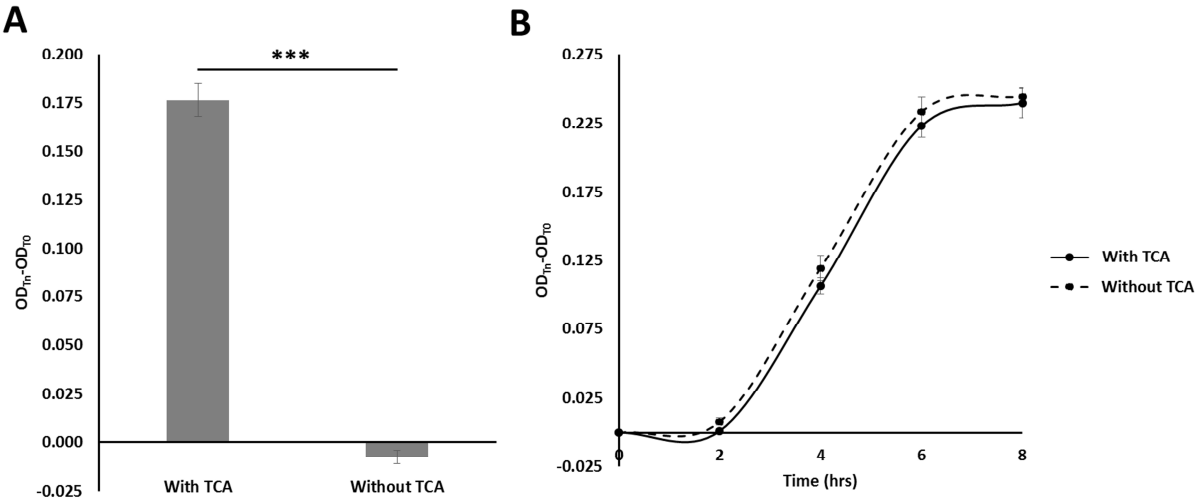

ACCEPTED MANUSCRIPT

ACCEPTED MANUSCRIPT

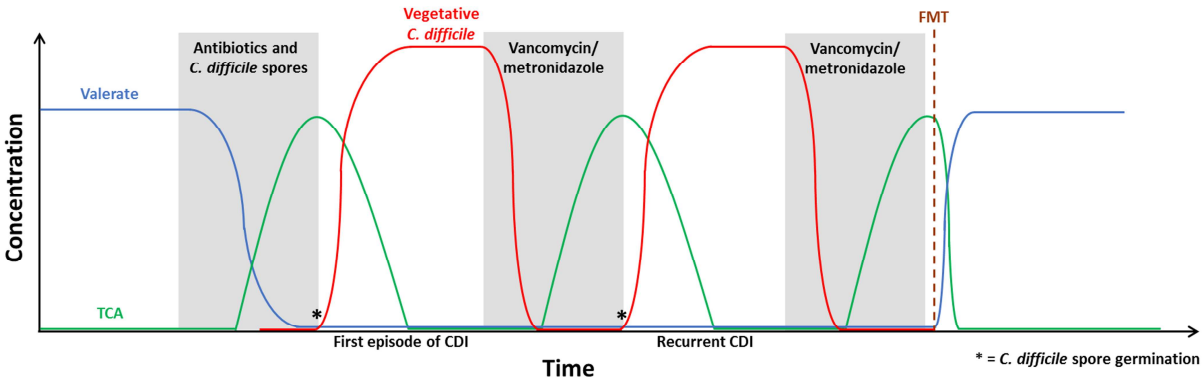

ACCEPTED MANUSCRIPT